Protist 173 (2022) 125868
http://www.elsevier.de/protis
Published online date 3 March 2022

Protist

Protist *Reviews*

Diplonemids – A Review on "New" Flagellates on the Oceanic Block[1]

Daria Tashyreva[a,2], Alastair G.B. Simpson[b], Galina Prokopchuk[a,c], Ingrid Škodová-Sveráková[a,d,e], Anzhelika Butenko[a,c,d], Michael Hammond[a,c], Emma E. George[f], Olga Flegontova[a,d], Kristína Záhonová[a,d,g], Drahomíra Faktorová[a,c], Akinori Yabuki[h], Aleš Horák[a,c], Patrick J. Keeling[f], and Julius Lukeš[a,c,2]

[a]Institute of Parasitology, Biology Centre, Czech Academy of Sciences, České Budějovice (Budweis), Czech Republic
[b]Department of Biology, Dalhousie University, Halifax, Canada
[c]Faculty of Science, University of South Bohemia, České Budějovice (Budweis), Czech Republic
[d]Faculty of Science, University of Ostrava, Ostrava, Czech Republic
[e]Faculty of Natural Sciences, Comenius University, Bratislava, Slovakia
[f]Department of Botany, University of British Columbia, Vancouver, Canada
[g]Faculty of Science, Charles University, BIOCEV, Vestec, Czech Republic
[h]Deep-Sea Biodiversity Research Group, Research Institute for Global Change, Japan Agency for Marine-Earth Science and Technology (JAMSTEC), Yokosuka, Japan

Submitted January 14, 2022; Accepted February 28, 2022
Monitoring Editor: Michael Melkonian

Diplonemids are a group of flagellate protists, that belong to the phylum Euglenozoa alongside euglenids, symbiontids and kinetoplastids. They primarily inhabit marine environments, though are also found in freshwater lakes. Diplonemids have been considered as rare and unimportant eukaryotes for over a century, with only a handful of species described until recently. However, thanks to their unprecedented diversity and abundance in the world oceans, diplonemids now attract increased attention. Recent improvements in isolation and cultivation have enabled characterization of several new genera, warranting a re-examination of all available knowledge gathered so far. Here we summarize available data on diplonemids, focusing on the recent advances in the fields of diversity, ecology, genomics, metabolism, and endosymbionts. We illustrate the life stages of cultivated genera, and summarise all reported interspecies associations, which in turn suggest lifestyles of predation and parasitism. This review also includes the latest classification of diplonemids, with a taxonomic revision of the genus *Diplonema*. Ongoing efforts to sequence various diplonemids suggest the presence of large and complex genomes, which correlate with the metabolic versatility observed in the model

[1] This review is one in a series on the biology of selected protist groups (see https://doi.org/10.1016/j.protis.2021.125818).

[2] Corresponding authors;
e-mails tashyreva@paru.cas.cz (D. Tashyreva), jula@paru.cas.cz (J. Lukeš).

https://doi.org/10.1016/j.protis.2022.125868

species *Paradiplonema papillatum*. Finally, we highlight its successful transformation into one of few genetically tractable marine protists.

Key words: Protists; taxonomic revision; ultrastructure; Euglenozoa; ecology; marine flagellates.

Contents

Introduction

Diplonemids (Diplonemea) are a group of heterotrophic, predominantly marine flagellates that belong to the phylum Euglenozoa and are closely related to the mostly parasitic kinetoplastid and free-living euglenid protists. The best-known diplonemids belong to the family Diplonemidae, including the genera *Diplonema* and *Rhynchopus.* Such cells are sack-shaped but highly plastic, capable of deformative movements similar to 'metaboly' seen in euglenids (Griessmann 1914; Schnepf 1994; Skuja 1948; Triemer and Ott 1990). Like most Euglenozoa they have a flagellar pocket and a tubular feeding apparatus, but between the two is an apical papilla that is distinctive for diplonemids.

For several decades, only cells confidently fitting this description were assigned to diplonemids, suggesting that the group had limited diversity. They were uncommonly encountered in nature and thus considered rare, often referred to as unusual euglenids, and only occasionally morphologically studied or included in comparative evolutionary frameworks. Just two genera of diplonemids, namely *Diplonema*, and *Rhynchopus*, each with only a few species, were described using classic protistology methods. Recently however, environmental molecular studies have revealed a wide range of diplonemid-related 18S rRNA gene sequences, especially in marine plankton communities, suggesting that the group is in fact highly diverse and present in virtually every marine niche including sediment layers (Boeuf et al. 2019; de Vargas et al. 2015; Flegontova et al. 2016, 2020; Gawryluk et al. 2016; Obiol et al. 2020; Schoenle et al. 2021). In addition, several new diplonemid species were recently isolated and described (Prokopchuk et al. 2019; Tashyreva et al. 2018a,b).

Diplonemids are compelling to study for their unusual cell and molecular biology, their potential to clarify evolutionary transitions within Euglenozoa, and their inescapable ecological importance. The phylogenetic position of diplonemids within Euglenozoa makes them crucial for understanding the cellular evolution of kinetoplastids and euglenids, which are both diverse and highly derived at molecular and cellular levels. This has motivated ultrastructural examinations of diplonemids (Montegut-Felkner and Triemer 1996; Prokopchuk et al. 2019; Tashyreva et al. 2018a,b), description of RNA editing and *trans*-splicing in their reticulated mitochondrion (Burger and Valach 2018; Kaur et al. 2020; Valach et al. 2017; Yabuki et al. 2016), analysis of their modified peroxisome (Makiuchi et al. 2011; Morales et al. 2016), determination of their endosymbionts (George et al. 2020), and overall metabolism (Škodová-Sveráková et al. 2021). While

we have learned a lot about these and few other features of diplonemids, we still know surprisingly little about their nuclear genome, lifestyle, and ecology. Nonetheless, diplonemids already proved to be molecular evolutionary enigmas in their own right. The most spectacular example is their mitochondrial genome, which likely represents the biggest organellar genome known to date (Lukeš et al. 2018).

The ecology of diplonemids is not well understood, but various data indicate important and/or unusual ecological roles. Marine planktonic diplonemids show exceptionally high relative abundances in environmental sequence datasets, in addition to astonishing 'molecular species' diversity (Flegontova et al. 2016, 2020; Gawryluk et al. 2016; Obiol et al. 2020; Schoenle et al. 2021), suggesting both a high abundance of cells, and highly diverse ecological functions. However, their lifestyles and feeding strategies remain mostly enigmatic, with eukaryote-proximal isolations of diplonemids suggesting roles in predation and/or parasitism on diatoms and other protists, as well as copepods, lobsters and plants (Elbrächter et al. 1996; Kent et al. 1987; Porter 1973; Schoenle et al. 2021; Triemer and Ott 1990). Diplonemids also stand out amongst (nominally) free-living heterotrophic flagellates by being highly amenable to cultivation (Nerad 1990; Schuster et al. 1968; Tashyreva et al. 2018a). A range of Diplonemidae and Hemistasiidae are available as axenic cultures, and some can grow to high densities, making them valuable for various comparative cell and molecular biological studies.

This review aims to introduce the basic biology of diplonemids, including their cell structure and life histories, metabolism, behavior and endosymbiotic bacteria, as well as our emerging understanding of their molecular biology and insights from genomic data. It also presents a current view of the phylogenetics and systematics of diplonemids and describes their known and inferred ecological roles. Moreover, we describe recent progress in genetic manipulations of diplonemids, which promises to turn these abundant marine biflagellates into new research models.

Large-scale Phylogeny

Several morphological similarities, such as the structure and properties of the feeding apparatus and presence of tubular extrusomes clearly pointed to diplonemids being related to euglenids and/or kinetoplastids, that is, the taxa now united as Euglenozoa (Kivic and Walne 1984; Schuster et al. 1968; Skuja 1948; Triemer and Ott 1990). The formal proposal of Diplonemia/Diplonemea as a third major taxon of Euglenozoa dates to 1993 (Cavalier-Smith 1993) and has generally been accepted since (Simpson 1997). Molecular phylogenetic support was later provided using both mitochondrial (cytochrome *c* oxidase subunit I) and nuclear (18S rRNA) markers (Maslov et al. 1999).

Early accounts based on light and electron microscopy usually, if tentatively, regarded diplonemids as closely affiliated with euglenids, either as an unusual euglenid (Schuster et al. 1968; Skuja 1948), or later, as a sister group to euglenids (Kivic and Walne 1984). By contrast, the majority of molecular phylogenies, mostly based on the 18S rRNA gene or heat shock proteins, favored a diplonemid-kinetoplastid clade (Breglia et al. 2007; Simpson et al. 2002, 2004; Simpson and Roger 2004). The poor taxon sampling in early analyses, plus the divergent nature of euglenozoan 18S rRNA gene sequences gave some reason to doubt the diplonemid-kinetoplastid relationship, and several studies indeed showed alternative topologies (Busse and Preisfeld 2002; Moreira et al. 2001; Yubuki et al. 2009). Nonetheless, recent multigene phylogenies do convincingly support diplonemids as being more closely related to kinetoplastids than to euglenids (Butenko et al. 2020; Lax et al. 2021). In parallel it was established that diplonemids possess a glycosome similar to kinetoplastids (Morales et al. 2016). Based on this shared presence of glycosomes, Cavalier-Smith (2016) proposed a subphylum Glycomonada containing Diplonemea and Kinetoplastea.

Prior to 2015, the only taxa assigned confidently to diplonemids were *Diplonema* (Griessmann 1914), and *Rhynchopus* (Skuja 1948), with a handful of species known for each genus. Their monophyly was first shown by Busse and Preisfeld (2002) and was confirmed in all subsequent molecular phylogenetic studies. These taxa are currently referred to as 'classic diplonemids' and grouped into the family Diplonemidae (Kostygov et al. 2021). In recent years the described genus and species diversity of classic diplonemids has expanded markedly, through formal descriptions of cultures established several decades earlier (Nerad 1990), and a multiple novel isolates. Two previously unknown species of both *Diplonema* (*D. japonicum, D aggregatum*) and *Rhynchopus* (*R. humris, R. serpens*), as well

as two new genera (*Lacrimia* and *Sulcionema*), were established recently (Tashyreva et al. 2018a, b). *Lacrimia lanifica* represents the only cultivated member of a clade that also contains numerous environmental sequences, showing that a significant part of diplonemid diversity is yet to be discovered. *Flectonema neradi*, initially referred to as *Diplonema* sp. 2/ATCC 50224 (Maslov et al. 1999; Nerad 1990), was established as a separate genus within Diplonemidae based on 18S rRNA-based phylogenies (Tashyreva et al. 2018a,b). Together with *Sulcionema specki*, they form the basal-most clades within this family, with no records from environmental sequencing surveys (Kostygov et al. 2021).

In 2015, 18S rRNA gene phylogeny convincingly showed that the euglenozoan taxon *Hemistasia* (Griessmann 1914) represents another diplonemid lineage (Yabuki and Tame 2015). *Hemistasia* had been considered as a possible relative of diplonemids based on light microscopy (Patterson et al. 2000), and although it was placed within kinetoplastids in the first ultrastructural study (Elbrächter et al. 1996), these same data hinted strongly at a close affinity with diplonemids (Simpson 1997; Simpson and Roger 2004). Consequently, Hemistasiidae was established as the second diplonemid family alongside Diplonemidae (Cavalier-Smith 2016). Shortly afterwards, *Namystynia karyoxenos* and *Artemidia motanka* were described and on the basis of ultrastructural features and 18S rRNA gene sequences were robustly placed in Hemistasiidae (Prokopchuk et al. 2019).

In 2001, a seminal study in environmental sequencing of eukaryotes revealed the existence of protists related to diplonemids in samples from the Southern Ocean (López-García et al. 2001). This discovery was somewhat overshadowed by the parallel description of high diversity and abundance of marine alveolates in the same work. However, a follow-up study confirmed the existence of two diplonemid-related environmental clades with a pan-oceanic distribution in deep-sea plankton samples and named them Deep Sea Pelagic Diplonemids (DSPD) I and II (Lara et al. 2009). DSPD I diplonemids were then formally established as the family Eupelagonemidae, with a one species *Eupelagonema pacifica,* described from a single cell isolate (Gawryluk et al. 2016; Okamoto et al. 2019). Interestingly, eupelagonemids are by far the most diverse and abundant lineage of Diplonemea and the most diverse lineage of planktonic eukaryotes in general (Flegontova et al. 2016; Flegontova et al. 2020). Despite their enormous diversity, when compared to other diplonemid families, eupelagonemid 18S rRNA genes show rather low divergence, suggesting their relatively recent rapid radiation (Flegontova et al. 2016; Gawryluk et al. 2016; Okamoto et al. 2019). In spite of our significant efforts, no representatives of DSPD II have been brought into culture, nor isolated and characterized by light microscopy.

The cladogram summarizing the current understanding of diplonemid phylogeny is shown in Figure 1. Class Diplonemea (or diplonemids) is divided into four clades - the families Diplonemidae (or classic diplonemids), Hemistasiidae, and Eupelagonemidae (previously known as DSPD I), and the undescribed environmental clade DSPD II. In all recently published phylogenies, Diplonemidae

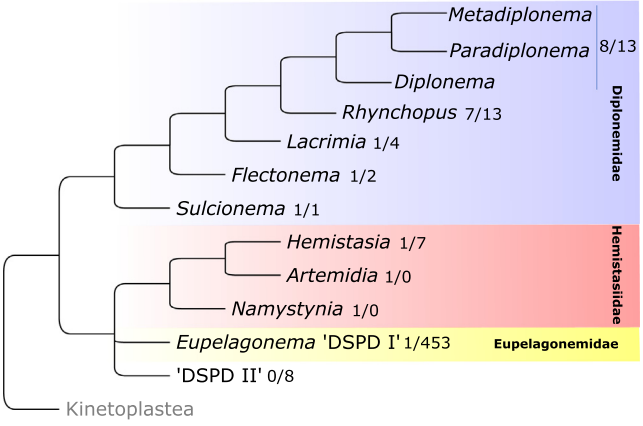

Figure 1. A cladogram showing phylogenetic relationships among diplonemid lineages based on 18S rRNA gene sequences. Kinetoplastea is used as an outgroup. Numbers by each taxon indicate how many species were formally described/number of 18S rRNA gene sequences deposited in EukRef database.

branch as a sister group to the other clades (Okamoto et al. 2019; Prokopchuk et al. 2019; Tashyreva et al. 2018a,b; Yabuki et al. 2021), but the remaining branching order is not stable and varies between studies (Gawryluk et al. 2016; Okamoto et al. 2019; Tashyreva et al. 2018a,b). Moreover, a recent 18S rRNA phylogeny does not retrieve the monophyly of Hemistasiidae sensu Prokopchuk et al. (2019), and merges DSPD II, Eupelagonemidae, and Hemistasiidae into a single clade called 'DSPDH' (Yabuki et al. 2021). Apparently, the 18S rRNA genes lack the information to resolve deep diplonemid evolution, and until representative genomic data are available across Diplonemea to allow more robust multigene phylogenies, this question remains open.

Small-scale Phylogeny and Taxonomic Revision of the Genus *Diplonema*

The genus *Diplonema* was established by Griessmann (1914) on the basis of light microscopy observations to accommodate an unusual colorless biflagellated marine protist, with elongated body tapering anteriorly, and capable of gliding and metabolic movement; the species was described as *D. breviciliata*. Later, two similar colorless highly metabolic biflagellates were characterized by light and electron microscopy, placed into a new genus *Isonema*, and designated as *I. nigricans* (Schuster et al. 1968) and *I. papillatum* (Porter 1973). After this, Larsen and Patterson (1990) described two other *Diplonema* species based on light microscopy alone; *D. ambulator*, which was very similar to *D. breviciliata*, but smaller, and *D. metabolicum,* which resembled *I. nigricans*. At the same time, Triemer and Ott (1990) characterized an organism that they identified as *D. ambulator* (though we regard it as a different species since it is freshwater, while *D. ambulator* is marine; see below), sharing a close morphological resemblance to *D. breviciliata* and a high similarity to *Isonema* spp. at the ultrastructural level. Due to this similarity, Triemer and Ott (1990) considered *Isonema* to be a junior synonym of *Diplonema* and transferred *I. papillatum* and *I. nigricans* into the genus *Diplonema*.

Further studies of the family Diplonemidae supported the underlying similarity of all of its members at the ultrastructural level, but also pointed out that there were substantial differences in morphology, life history characteristics and motility modes (Nerad 1990; Tashyreva et al. 2018a,b). Furthermore, the genus *Diplonema* sensu lato was found paraphyletic relative to *Rhynchopus* by some (von der Heyden et al. 2004). Our maximum likelihood phylogeny of diplonemids with focus on *Diplonema* (sensu lato) (Fig. 2), as well as the pairwise-distances matrix of the 18S rRNA gene (Supplementary Material Table S1) suggest sufficient genetic separation to justify the division of *Diplonema* into three new genera: *Diplonema, Metadiplonema*, and *Paradiplonema*. The first group is comprised of five unique sequences sharing 93.5 to 97.7% similarity (Supplementary Material Table S1) and forming a well-supported clade (Fig. 2), hereafter designated as the genus *Diplonema* (sensu stricto). We also include Griessmann's (1914) non-sequenced *D. breviciliata*, which closely resembles sequenced *Diplonema* sensu stricto isolates in terms of morphology and behavior, as well as a freshwater species identified as *D. ambulator*, which is additionally supported by highly similar ultrastructure (see below). The second clade is represented by "*Isonema*" ATCC 50232, which is morphologically similar to *I. nigricans* (Nerad 1990), and a 94.1% similar environmental sequence (Supplementary Material Table S1), sharing 85.9 to 89% similarity with *Diplonema* sensu stricto, and hereafter designated as the genus *Metadiplonema* (Fig. 2). The third clade contains a single sequence of the species previously known as '*Isonema papillatum*' or '*Diplonema papillatum*', which has so far served as a model organism for diplonemids. This shares 86.6 to 88.3% similarity with *Diplonema* sensu stricto and 84.2 to 87.7% with *Metadiplonema* and is hereafter designated as the type of the genus *Paradiplonema* (Fig. 2).

This subdivision is supported by life history stages, motility modes and morphological traits that are highly consistent within each genus. Life stages include trophic behavior under nutrient-available conditions, and other stages induced by starvation. Differences in motility include gliding or oscillating swimming under trophic conditions. Morphological traits include the shape of body, the size of C-shaped collar encircling the cytostome, the size of apical papilla, the presence of additional quadratically packed bundles of microtubules at the proximal part of the cytopharynx below the bottom of the flagellar pocket and the presence of extrusomes in the trophic and swimming stages. Moreover, the phylogenetic tree suggests the presence of two putative novel genera within the *Diplonema* sensu lato clade

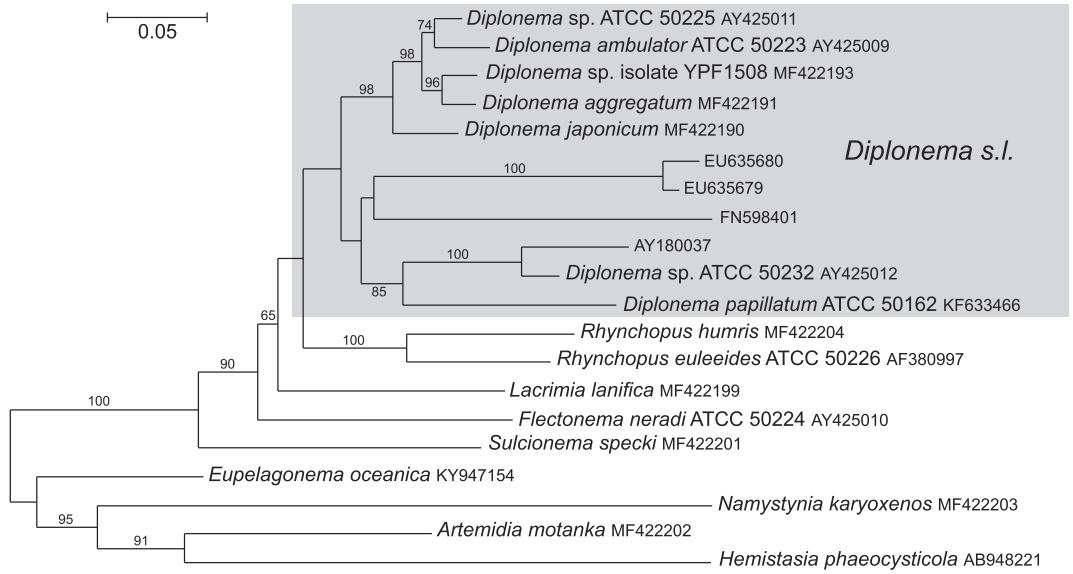

Figure 2. The 18S rRNA-based maximum likelihood phylogeny of diplonemids with focus on *Diplonema* s.l. The final data matrix comprising 20 taxa and 1999 aligned nucleotide positions was analyzed using the GTR + G4 model in RAxML 8. Numbers above the branches refer to non-parametric bootstrap support (of values 50 and higher) inferred from 500 replicates in RAxML 8. For sequences from uncultured specimens, only the NCBI accession numbers are shown.

(<86% 18S rRNA gene similarity to aforementioned clades). Since they are represented by three environmental sequences (EU635679, EU635680, and FN598401), and thus lack any morphological data (Fig. 2; Supplementary Material Table S1), we refrain from further comments on their taxonomic status. The list of partially and formally described species is available as Supplementary Material Table S2.

Genus *Diplonema* Griessmann 1914

Features based on Griessmann 1914; Larsen and Patterson 1990; Nerad 1990; Triemer and Ott 1990; Montegut-Felkner and Triemer 1996; Tashyreva et al. 2018b: trophic stage with a slender elongated body with constricted anterior end. Deep subapical flagellar pocket. Two equal to subequal flagella a third of the body length, lacking paraflagellar rods (PFR), inserted at 45° relative to the longitudinal cell axis. Gliding motility accompanied by slow movement ("ambulation") of flagella. Well-developed C-shaped collar; proximal part of the cytopharynx supported by additional quadratically packed bundles of microtubules. Extrusomes absent. Starvation-induced transient sessile stage further transforming into the swimming stage with extrusomes and long flagella supported by the PFR. Anterior flagellum forming a lasso, posterior flagellum stretched along the body. Fast swimming.

Type species: *Diplonema breviciliata* Griessmann 1914

Composition: *D. ambulator*, *D. japonicum*, and *D. aggregatum* (molecular data, morphology, motility pattern and life cycles); *D. breviciliata* (morphology and motility pattern); a freshwater species referred to as "*Diplonema ambulator*" by Triemer and Ott (1990) (morphology and motility pattern); *Diplonema* sp. ATCC 50225 (molecular data, morphology, motility pattern and life cycles); *Diplonema* spp. YPF1508 (molecular data); *Diplonema* spp. ATCC 50222 and XIICD (morphology, motility pattern and life cycles).

Genus *Metadiplonema* nom. nov. (Tashyreva, Simpson, Horák and Lukeš)

Features based on Schuster et al. 1968 and Nerad 1990.

Description: The trophic stage with broad anterior quarter tapering posteriorly into a fine tip, exhibiting gliding motility. Two equal short flagella lacking the PFR, inserted subapically. Extrusomes present in the trophic stage. Very reduced C-shaped collar and small apical papilla. Lacks additional bundles of microtubules at the proximal end of the cytophar-

ynx. Starvation-induced fast-swimming stage with anterior flagellum forming a lasso and posterior flagellum stretched along the body, not studied at the ultrastructural level. Transient sessile stage not known.

Type species: *Metadiplonema nigricans* Schuster et al. 1968 (comb. nov.)

Etymology: The generic name (neuter from Greek "meta" meaning "after") reflects relatedness to *Diplonema*.

Composition: *Metadiplonema nigricans* comb. nov. (morphology and motility) and *Metadiplonema* sp. ATCC 50232 (molecular data, morphology, motility pattern and life cycles).

Notes: *Metadiplonema* is a nomen novum to replace *Isonema* Schuster et al. (1968), who did not explicitly state whether they were describing their new genus under the zoological code or botanical code, but given its form (e.g., lack of a Latin description), we assume they intended to describe it under the zoological code. *Isonema* Schuster et al. 1968 appears to be a junior homonym in zoological nomenclature, with *Isonema* (Meek and Worthen 1865, 1868) being a fossil gastropod (*Isonema* also has a botanical homonym in *Isonema* Brown (R.Br.) 1810, an angiosperm). In accordance with the recommendations of the International Code of Zoological nomenclature (Art. 60, 67.8), we have nominated the same type species for *Metadiplonema* as was nominated for *Isonema* by Schuster et al. 1968 (*Isonema nigricans* = *Metadiplonema nigricans* comb. nov.), making *Metadiplonema* and *Isonema* Schuster et al. 1968 objective synonyms.

Genus *Paradiplonema* gen. nov. (Tashyreva, Simpson, Horák and Lukeš)

Description: elongated trophic stage characterized by slow oscillating swimming within the water column, lacks extrusomes. Short equal flagella inserted slightly subapically, do not form anterior lasso, and lack the PFR. Gliding motility absent. Highly reduced C-shaped collar and well-developed apical papilla. Additional bundles of microtubules at proximal end of the cytopharynx absent. Does not transform into fast-swimming stage under nutrient limitation.

Type species: *Paradiplonema papillatum* Porter 1973 comb. nov.

Etymology: the generic name comes from the Greek prefix "*para*" meaning "adjacent", pointing to the close relationship to the genus *Diplonema*.

Composition: *Paradiplonema papillatum* ATCC 50162 (molecular data, morphology, motility pattern and life cycles), *Paradiplonema* sp. ATCC 50227 and *Paradiplonema* sp. ATCC 50228 (morphology, motility pattern and life cycles).

Light Microscopy

Diplonemids are relatively large flagellates ranging from 10 to 30 μm in length (Tashyreva et al. 2018a), with two species exceeding 30 μm (Larsen and Patterson 1990; Schuster et al. 1968). Their bodies are sac-shaped and very plastic, exhibiting frequent metabolic contortions (Fig. 3K). This unifying feature of Diplonemidae and Hemistasiidae is seemingly missing in eupelagonemids, which have rigid bodies (Gawryluk et al. 2016; Okamoto et al. 2019). Most diplonemids are characterized by cylindrical or flattened bodies (Fig. 3A, B, D-F, H, I, K), often constricted anteriorly (Fig. 3A-I, K), and sometimes at the posterior end (Fig. 3J) (Elbrächter et al. 1996; Nerad 1990; Prokopchuk et al. 2019; Tashyreva et al. 2018a), with the exception of *Lacrimia* featuring a teardrop-shaped body (Fig. 3G) (Tashyreva et al. 2018a). In addition to differentiation into life stages (see Life Cycles section), many species display high variability in cell size within a single trophic culture. This is especially pronounced in *P. papillatum* and *S. specki* and hemistasiids, which are also greatly variable in shape (Fig. 3A-D) (Elbrächter et al. 1996; Porter 1973; Prokopchuk et al. 2019; Tashyreva et al. 2018a). Hemistasiids change their shape from cylindrical to teardrop/pyriform due to the presence of a large posterior digestion (Elbrächter et al. 1996) or lipid vacuole (Fig. 3C; our unpublished data). Smaller cytoplasmic lipid-like inclusions are localized predominantly at the posterior half in all trophic Diplonemidae and Hemistasiidae (Fig. 3C, D, F, H) but diminish or disappear during starvation (Prokopchuk et al. 2019; Tashyreva et al. 2018a). Sometimes the inclusions are distributed throughout the cytoplasm (Fig. 3I) or localized anteriorly (Fig. 3G). All diplonemids are colorless, although one species, *M. nigricans*, contains sepia-colored cytoplasmic granules that are excreted into the medium (Schuster et al. 1968). The characteristic apical papilla, J-shaped cytopharynx, deep flagellar pocket, batteries of extrusomes and hemistasiid lacunae can be also seen at the light microscopy level (Fig. 3D, E). Distinguishing morphological features of each genus have been recently summarized elsewhere (Kostygov et al. 2021).

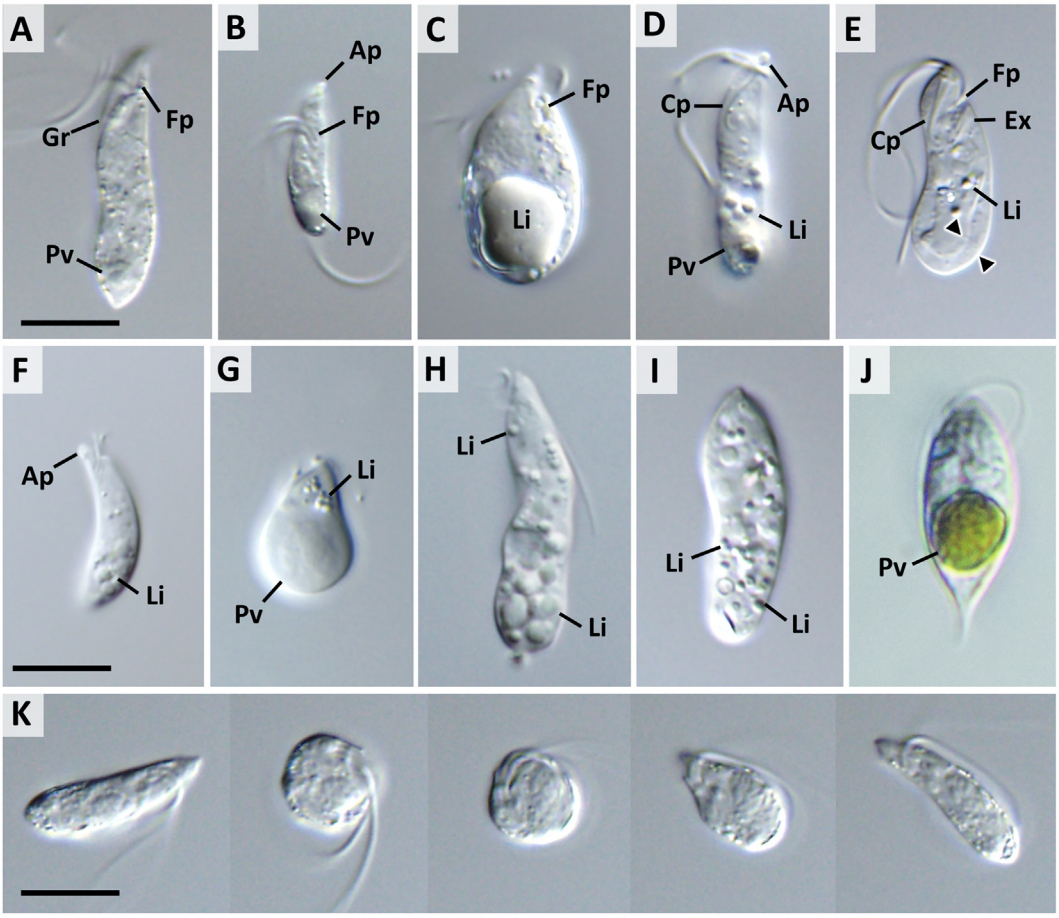

Figure 3. A-D. Differential interference contrast micrographs of *Namystynia karyoxenos* illustrating morphological variability within a single culture. Large (**A**), small (**B**) and medium-sized (**D**) cells with different amount of lipid-like cytoplasmic inclusions (*Li*), and a large teardrop-shaped cell with a prominent posterior lipid vacuole (**C**). Note subapical localization of deep flagellar pocket (*Fp*), asymmetrical apex with anterior groove (*Gr*) and apical papilla (*Ap*), and various sizes of posterior vacuoles (*Pv*). **E.** *Artemidia motanka* with indicated cytopharynx (*Cp*), flagellar pocket, battery of extrusomes (*Ex*) and swollen lacunae (between *arrows*). **F-I.** Cultured cells of Diplonemidae species under nutrient-rich conditions. **F.** Elongated crooked cell of *Flectonema neradi* with posterior *Li*. **G.** Teardrop-shaped cell with a large posterior vacuole occupying most of the cell volume and small anterior *Li*. **H.** *Sulcionema specki* with predominantly posterior *Li*. **I.** Trophic *Rhynchopus euleeides* with *Li* scattered throughout the cell. **J.** Environmental eupelagonemid with posterior constricted to a fine tip and a large posterior food vacuole (*Pv*) and lacking cytoplasmic granulation. **K.** Time-lapse images of *N. karyoxenos* displaying metaboly Scale bars: 10 μm.

Ultrastructure

All diplonemids studied to date share a broadly similar ultrastructural organization. Their smooth sac-shaped bodies lack pellicles and extracellular skeletal elements. The plasma membrane is subtended by a corset of interlinked microtubules (Figs 4A-C, 5A, B). These microtubules are more or less evenly spaced and arranged in parallel, enclosing the entire cell in a helical manner (Fig. 4B) (Porter 1973; Prokopchuk et al. 2019; Tashyreva et al. 2018a). Sacs of rough or smooth endoplasmic reticulum (ER) are often seen either immediately beneath the microtubular corset (Fig. 4C) or over branches of the mitochondrion. Hemistasiids possess an expanded membrane-bound compartment called the lacuna (Fig. 4F, G, J), which lies directly underneath the microtubular corset over most of the cell body (Fig. 4G) (Elbrächter et al. 1996; Prokopchuk et al. 2019), possibly representing an unusually extensive form of the endomembrane system.

The single reticulated mitochondrion occupies large portions of the cell periphery (Fig. 4D, G;

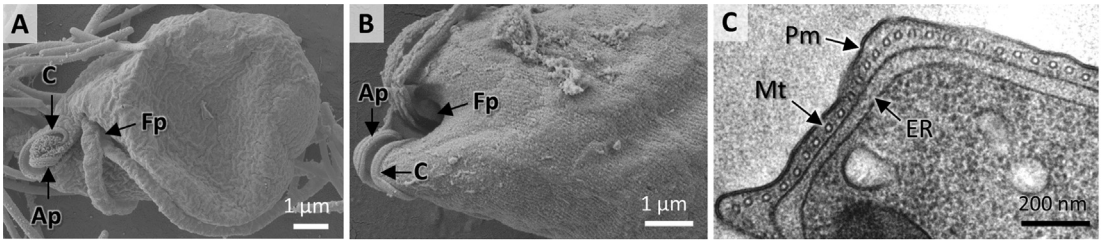

Figure 4. A. SEM image of *Artemidia motanka* showing smooth surface and pronounced apical asymmetry. **B**. SEM image of *Lacrimia lanifica* with less pronounced apical asymmetry and dense microtubular corset apparent through the plasma membrane. **C.** TEM image through cortical layer of *Diplonema aggregatum* with peripheral microtubular corset (*Mt*) under plasma membrane (*Pm*) and underlying smooth endoplasmic reticulum (*ER*). *Ap* – apical papilla, *C* – C-shaped collar, *Fp* – flagellar pocket.

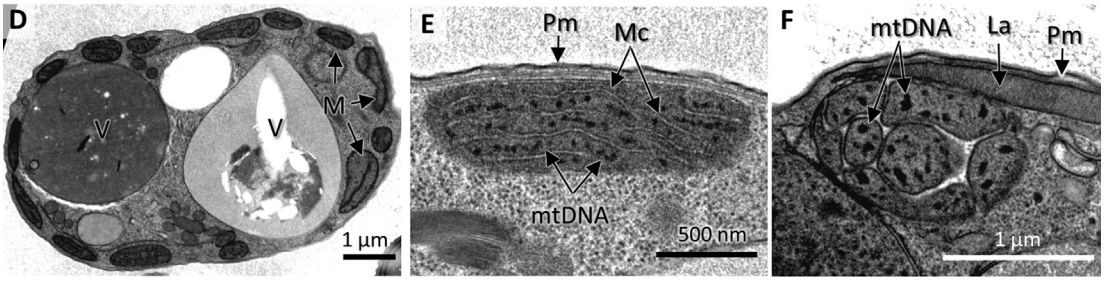

D. Obliquely sectioned trophic cell of *Rhynchopus serpens* showing peripheral mitochondrion. **E**. Close view of mitochondrial branch in *R. serpens*. **F.** Unusual arrangement of mitochondrial cristae in *A. motanka*. *La* – lacunae, *M* – mitochondria, *Mc* – mitochondrial cristae, *mtDNA* – mitochondrial DNA, Mt – microtubular corset, *Pm* – plasma membrane, *V* – vacuoles.

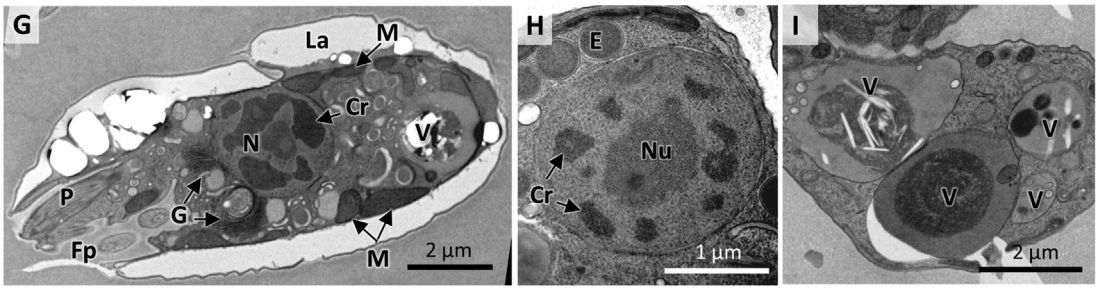

G. Longitudinal section through the entire cell of *Namystynia karyoxenos* showing position of main cellular structures and organelles. **H**. The nucleus of *Diplonema japonicum*. **I.** Multiple vacuoles of various size and content in *Sulcionema specki*. *Cr* – heterochromatin; *E* – endosymbiont; *Fp* – flagellar pocket, *G* – Golgi bodies, *La* – lacunae, *M* – mitochondria, *P* – cytopharynx, *N* – nucleus, *Nu* – nucleolus, *V* – vacuoles.

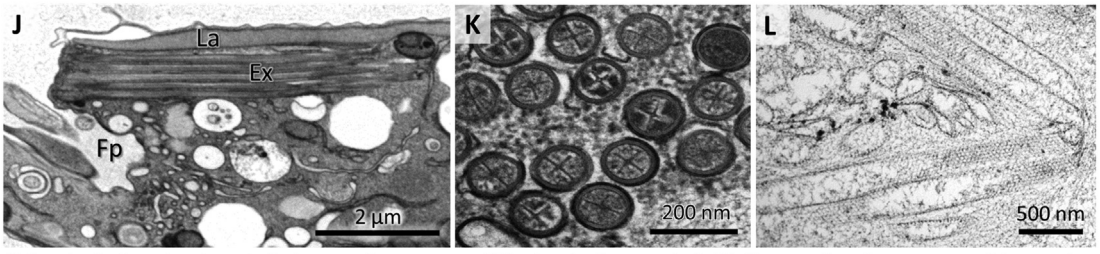

J. Longitudinal section through the battery of extrusomes of *Hemistasia phaeocysticola*. **K**. Cross-sectioned extrusomes of *A. motanka*. **L.** Extrusomes discharged from the swimming stage of *D. japonicum*. *Ex* – extrusomes, *Fp* – flagellar pocket, *La* – lacunae.

Figure 4. Scanning and transmission electron micrographs of selected diplonemid species showing common subcellular structures and organelles.

Tashyreva et al. 2018a). Most species have broad lamellar cristae, which mostly form stacks that tend to be parallel to the cell surface and have very limited connections to the inner mitochondrial membrane (Fig. 4D, E) (Marande et al. 2005; Prokopchuk et al. 2019; Tashyreva et al. 2018a,b). However, other species show smaller or more disordered cristae or instead have extensive connections to the inner mitochondrial membrane (Bodammer and Sawyer 1981; Elbrächter et al. 1996), and finally, some species are almost devoid of cristae (Schnepf 1994). Large electron-dense aggregates

of mitochondrial DNA are distributed throughout the matrix, interspersed between the cristae (Fig. 4E, F) (Lukeš et al. 2018).

The subspherical nucleus and several Golgi bodies, each formed by multiple stacks, are positioned either centrally or in the anterior half of the cell (Fig. 4G). The nucleus contains a large nucleolus and prominent electron-dense masses of heterochromatin (Fig. 4G, H). The nuclear envelope remains closed during mitosis (Triemer 1992). The cytoplasm is full of free ribosomes, tubules of rough and smooth ER, vacuoles and vesicles of various size and content (Fig. 4D, I, J). Most diplonemids contain several small digestion vacuoles, while hemistasiids and *Lacrimia* often display a single large posterior vacuole, which gives their bodies a pear-shaped appearance (Fig. 3C, G) (Kostygov et al. 2021; Prokopchuk et al. 2019; Tashyreva et al. 2018a).

Several species possess euglenozoan-type tubular extrusomes (Elbrächter et al. 1996; Nerad 1990; Prokopchuk et al. 2019; Simpson 1997; Tashyreva et al. 2018b). These thick-walled tubular structures have a cruciform center when viewed in cross-sections (Fig. 4J, K), and measure 2.5–4 μm in length and 110–140 nm in diameter. They typically form parallel batteries (Fig. 4J) or less commonly, are loosely arranged at slightly different angles, and are located mostly in the anterior half of the cell, adjacent to the flagellar pocket and occasionally, in the central region (Prokopchuk et al. 2019; Schuster et al. 1968; Tashyreva et al. 2018b). Discharged extrusomes expand several-fold in length and appear as hollow lattice cylinders (Fig. 4L). Extrusomes are invariably present in *Hemistasia* and *Artemidia*, and *Metadiplonema* ATCC 50232 and *M. nigricans* (Nerad 1990; Prokopchuk et al. 2019; Schuster et al. 1968). By contrast, in *Namystynia*, they are induced only by starvation (Prokopchuk et al. 2019) and are specific to the swimming and transient sessile stages of *D. japonicum*, *D. ambulator* and *D. aggregatum* (Nerad 1990; Tashyreva et al. 2018b).

Diplonemids are characterized by an apical papilla that connects to both a near-apical cytostome and a deep subapical flagellar pocket (FP), giving the cell anterior an asymmetric appearance (Figs 4A, B, G, 5B). This asymmetry is especially pronounced in hemistasiids because the FP lies in a depression further down the cell (Fig. 4A, G); this protruding apical part above the FP was also referred to as the rostrum (Elbrächter et al. 1996). Hemistasiids, *Lacrimia* and *Flectonema* are additionally distinguished by a pronounced spiral groove, which starts at the FP and runs halfway down the cell (Fig. 4A).

The ridge of the papilla is reinforced with several elements, most notably the MTR ('reinforced microtubules') that originates from the FP extension (Fig. 5F, H; see below). While most diplonemids feature a prominent tongue-shaped papilla (Fig. 5B), species of *Lacrimia*, *Rhynchopus* and *Flectonema* have a smaller and more narrow lip-like papilla (Fig. 5A). In hemistasiids, *Rhynchopus* and *Diplonema* species, the entire apical part of the cell is covered with a dense coat of fine hair (Fig. 5C, Q, R; Elbrächter et al. 1996; Prokopchuk et al. 2019; Tashyreva et al. 2018a,b).

The feeding apparatus (FA) itself opens as a cytostome encircled by a C-shaped rigid collar (Fig. 5A, B) consisting of a semi-circle of microtubules embedded in a dense matrix (Fig. 5K). The FA then extends as a long, tubular cytopharynx (Fig. 5A, J), which is usually positioned obliquely relative to the cell longitudinal axis. The cytopharyngeal lumen is reinforced by an ensemble of supporting elements, including four electron-dense folds with more diffuse coatings, called vanes (Fig. 5L, M). These are assembled in a partial rosette, each anchored near its base by a single microtubule. A lamellar structure with a different appearance runs alongside this rosette and is counted as a fifth vane. The vane-supporting microtubules are continuous with some from the MTR of the FA and papilla (Fig. 5H; see below). Several other elements run parallel to the cytopharynx, including rods made of amorphous material, other rows of longitudinal microtubules, and additional solitary microtubules (Fig. 5L, M). The most prominent, peripheral microtubular ribbon has a swirl-like appearance and directs away cytopharyngeal lumen-derived vesicles, (Fig. 5L; Montegut-Felkner and Triemer 1996). The pharyngeal complex is additionally encircled with sacs of smooth ER (Fig. 5L, M).

The cytopharynx initially runs more-or-less straight before taking a U-turn upwards (Fig. 5I, J), and sometimes makes further turns before it finally terminates (Montegut-Felkner and Triemer 1996). Before reaching the first turn, the peripheral microtubular ribbon disappears (Fig. 5J). At this point, the presence of supporting elements varies between species – the cytopharynxes of *D. aggregatum*, *D. japonicum*, *D. ambulator*, *Diplonema*

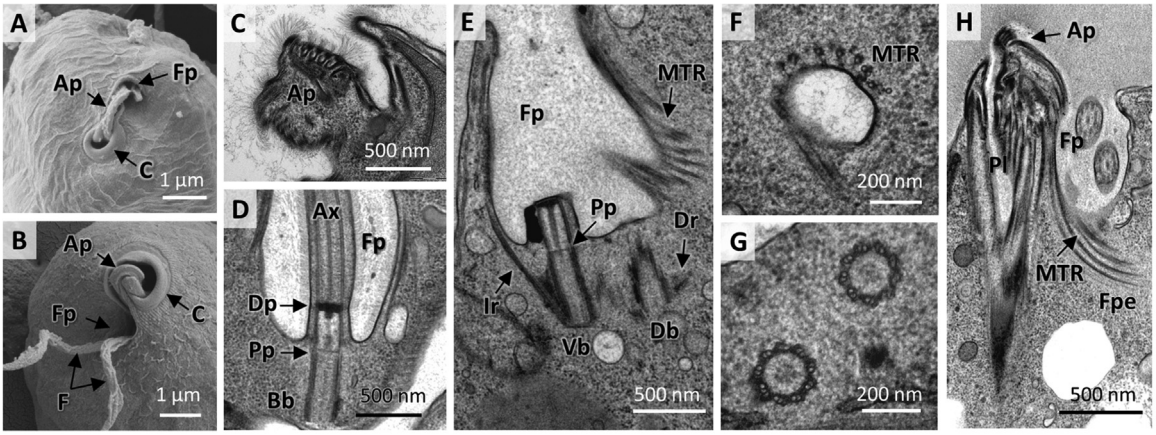

Figure 5. View at the cell apex of *Rhynchopus* sp. with a small lip-like papilla (*Ap*, **A**) and *Diplonema japonicum* with a well-developed tongue-shaped papilla (*Ap*, **B**); note subapical flagellar pocket (*Fp*) and well-developed C-shaped collar (*C*) encircling the cytostome. **C**. Dense hair covering the apical papilla (*Ap*) of *Namystynia karyoxenos*. **D.** Longitudinal section through the flagellum of *Diplonema aggregatum*. Note the basal body (*Bb*), transitional zone (between *arrows*) delimited by proximal (*Pp*) and dorsal (*Dp*) plates, and the axoneme (*Ax*) above the distal plate, consisting of outer microtubular circle and central microtubules. **E**. Longitudinal section through flagellar pocket region of *Sulcionema specki,* showing the ventral basal body (*Vb*) associated with the posterior flagellum and anchored with intermediate flagellar root (*Ir*) ascending along the flagellar pocket and perpendicular ventral root (not shown); the dorsal basal body (*Db*) is associated with anterior flagellum and anchored with ascending dorsal root (*Dr*). **F.** Cross-sectioned flagellar pocket extension of *Diplonema japonicum* supported by a row of microtubules (*MTR*). **G.** Cross section through the basal bodies of *D. japonicum.* **H.** Continuous MTR in *D. japonicum* originating at flagellar pocket extension (*Fpe*), looping over apical papilla (*Ap*) and descending along the cytopharyngeal lumen (*Pl)*.

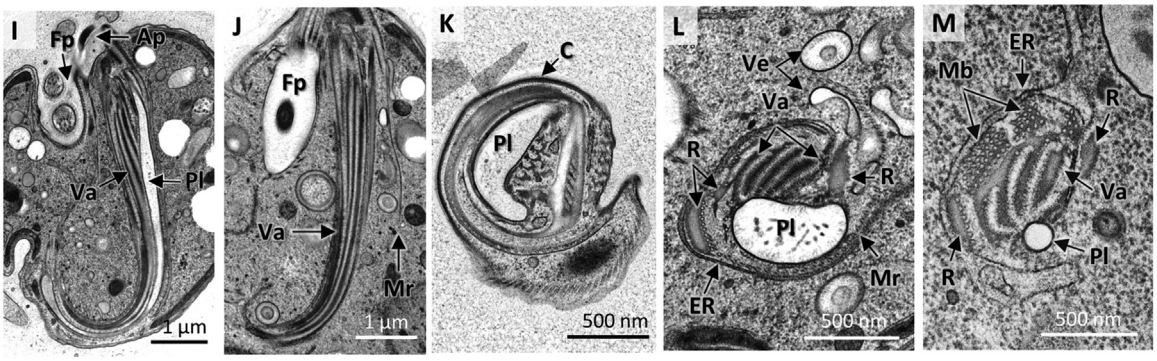

Longitudinal section through the horn-like cytopharynx of *D. aggregatum* (**I**) and *D. japonicum* (**J**) showing pharyngeal lumen (*Pl*), supporting vanes (*Va*) and peripheral ribbon of microtubules (*Mr*). **K-M**. Cross-sectioned feeding apparatus of *D. japonicum* through the cytostome (**K**) showing C-shaped collar (*C*), central region of the cytopharynx (**L**) and bottom of the pharynx before its J-turn (**M**). In **L**, note the supporting vanes (*Va*), vertical rods composed of amorphous material (*R*), outer microtubular ribbon (*Mr*), additional loosely arranged microtubules, vesicles (*Ve*) pinching off the pharyngeal lumen (*Pl*) and endoplasmic reticulum (*ER*) encircling the pharyngeal complex. Additional bundles of microtubules (*Mb*) appear at **M**, while outer microtubular ribbon disappears. Note amorphous matrix surrounding the supporting vanes (*Va*).

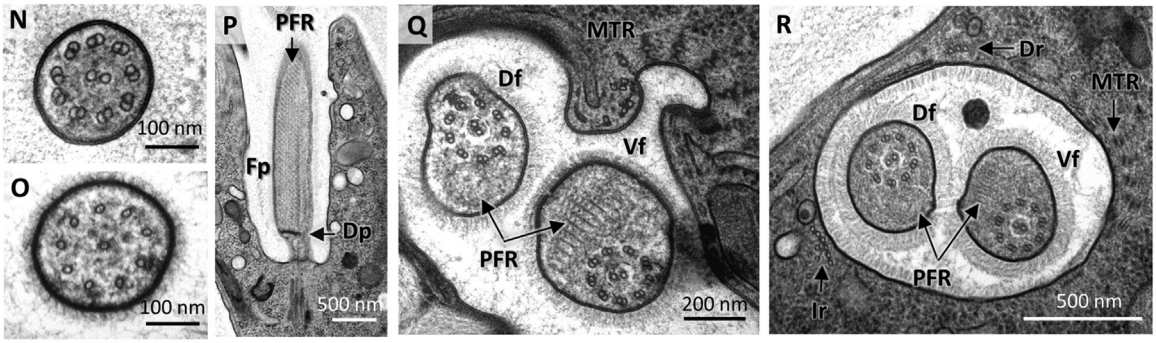

N. Cross-sectioned flagellum of *D. japonicum* in the trophic stage, displaying canonical 9+2 arrangement of microtubules. **O.** Cross-sectioned flagellum of *Rhynchopus* sp. in the trophic stage, showing nine outer singlets and a single central microtubule. **P.** Longitudinal section through the flagellar pocket (*Fp*) and the ventral flagellum of *D. japonicum* in the swimming stage; note the presence of paraflagellar rod (PFR) with a parallel lattice originating at the distal plate (*Dp*). **Q.** Cross-sectioned flagellar pocket of *N. karyoxenos*; note the *MTR* embedded into fibrous matrix by which it attaches to the plasma membrane, prominent *PFR* with parallel lattice in the ventral (posterior) flagellum (*Vf*) and smaller PRF with tubular lattice supporting the dorsal flagellum (*Df*). **R.** Cross-sectioned flagellar pocket of *D. japonicum* in the swimming stage; note the cross-sectioned dorsal (*Dr*) and intermediate roots (*Ir*), distinct structure of *PFR* in *Df* and *Vf,* and dense hair covering of both flagella and the flagellar pocket.

Figure 5. Scanning and transmission electron micrographs of cytopharyngeal and flagellar apparatuses in diplonemids.

ATCC 50225 and hemistasiids become associated with additional quadratically packed bundles of microtubules (Fig. 5M), whereas other diplonemids lack these (Montegut-Felkner and Triemer 1996; Nerad 1990; Prokopchuk et al. 2019; Tashyreva et al. 2018a,b).

Within the obliquely oriented FP, the two flagella arise from parallel basal bodies (Fig. 5G) that are joined by a fibrous connective (not shown; Montegut-Felkner and Triemer 1994). There are three flagellar microtubular roots: the dorsal root (DR or R3) originates near the outer side of the anterior basal body (F2/BB2) (Fig. 5E), while the intermediate root (IR or R1) commences from the interior side of the posterior basal body (F1/BB1) (Fig. 5E). The ventral root (VR or R2) is associated with the outer side of the posterior basal body, but may originate some distance away from it, at the cortical microtubule corset (Montegut-Felkner and Triemer 1994; Simpson 1997). The DR and IR ascend along the FP wall (Fig. 5E, R), with the VR projecting into the cytoplasm perpendicularly to the cell longitudinal axis (not shown). The FP wall is also subtended by the MTR, a row of evenly spaced microtubules, each reinforced with dense material by which it attaches to the plasma membrane (Fig. 5E, H, Q, R) (Montegut-Felkner and Triemer 1994). The MTR originates from the terminus of an often-deep J-shaped extension of the FP, runs along the entire length of the FP, and eventually becomes a supporting element of the apical papilla and cytopharynx (Fig. 5F, H). A connection between the distal end of the VR and the origin of the MTR is confirmed in at least one *Rhynchopus* species (Simpson 1997).

Most diplonemids have axonemes with the canonical 'nine doublets and a central pair' organization (Fig. 5N, Q, R), although the trophic stage of *Rhynchopus* species has short flagellar stubs enclosed within the FP, either with nine singlets and a single central microtubule (Fig. 5O), or several loosely arranged microtubules. The transition zone between the basal body and flagellar axoneme proper is delimited by a transitional transverse plate on each side (Fig. 5D, P). The two central axonemal microtubules penetrate through the distal plate, unlike in most other eukaryotic flagella (Montegut-Felkner and Triemer 1994).

Most diplonemids possess paraflagellar rods (PFRs; also known as paraxonemal rods) that resemble those in other Euglenozoa, with a parallel lattice in the posterior (ventral, F2) flagellum (Fig. 5P, Q, R), and a tubular lattice in the anterior (dorsal, F1) flagellum (Fig. 5Q, R). They originate at the distal transitional plate (Fig. 5P). The PFRs are permanently present in hemistasiids, *Lacrimia*, *Flectonema* and *Sulcionema*, and are most conspicuous in hemistasiids (Fig. 5Q). The PFRs appear only in the swimming stage of *Diplonema* spp. and *Rhynchopus* spp. (Fig. 5P, R; Tashyreva et al. 2018a,b), and presumably *Metadiplonema* spp. (Nerad 1990), coincident with flagellar lengthening, as well as the development of a canonical 9 + 2 axoneme in *Rhynchopus* spp. They appear to be entirely absent in *Paradiplonema* (Nerad 1990; Porter 1973).

Life Cycles

Depending on environmental nutrient availability, diplonemids exhibit different life stages (trophic, sessile and/or swimming), which are defined by distinct motility modes and the presence of characteristic morphological features (Fig. 6).

The trophic phase, which represents the dominant form under nutrient-rich conditions, is in *Diplonema*, *Metadiplonema*, and *Rhynchopus* defined by cells gliding along the surface, with active flagella being active if they emerge from the FP (Fig. 6A-C). All studied diplonemids gradually become smaller under nutrient-deprived conditions, with most species also undergoing morphological transitions. Under these cultivation conditions, *Rhynchopus* gradually transforms into the swimming stage, with the flagella extended beyond the FP, eventually attaining a length of more than twice the cell and developing PFR (Fig. 6A) (Roy et al. 2007; Simpson 1997; Tashyreva et al. 2018a). This swimming behavior is mediated by the 'spinning lasso' pattern of the dorsal flagellum around the anterior region (Nerad 1990; Roy et al. 2007; Tashyreva et al. 2018a), while the ventral flagellum is typically directed posteriorly (Fig. 6A, B).

By contrast, *Diplonema* species show two distinct stages of transformation when starved (Fig. 6B) (Nerad 1990; Tashyreva et al. 2018b). Gliding trophic cells will enter the sessile phase, which in these species serves as a transient period of modification into the swimming stage (Fig. 6B). Cells will take on a rounded, stationary appearance, sticking to surfaces through the acquisition of a mucilaginous coat (Fig. 6B). This period should not be confused for an encysted period of dormancy, as cells

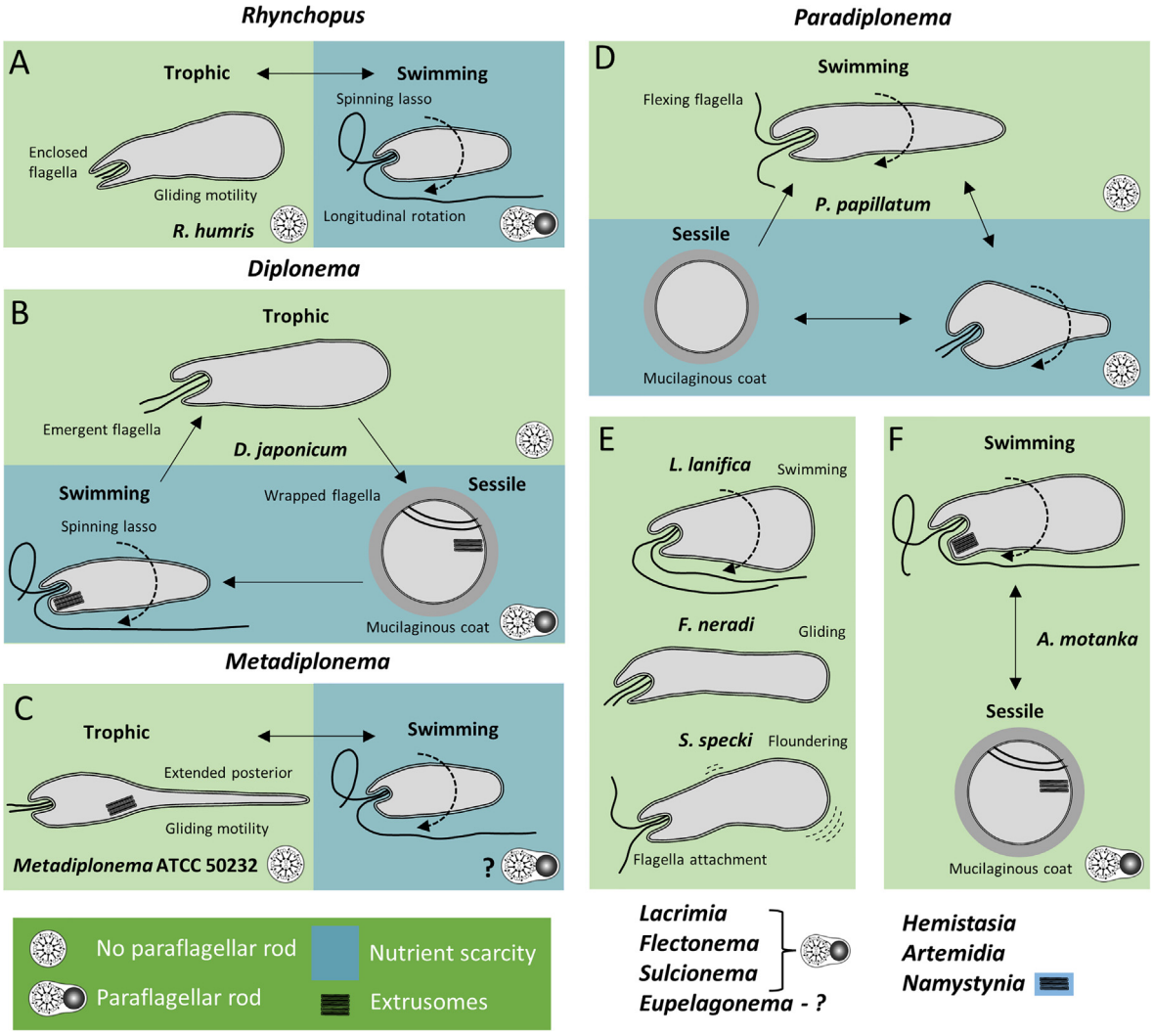

Figure 6. Schematic representation of life stages exhibited by cultured diplonemid genera showing relevant behavioral and morphological changes, including motility modes, flagella length as well as the presence of extrusomes and paraflagellar rods. Cells are not drawn to scale.

will pulsate with metabolic movements and rotate. During this stage, the flagella, already protruding from the FP, also gradually lengthen and thicken due to the construction of the PFR, while cells additionally develop tubular extrusomes (Fig. 6B). After a period of ~24-hour starvation or following the addition of nutrients to starved cells in the case of *D. aggregatum*, cells will emerge from the mucilaginous coat and begin swimming (Nerad 1990; Tashyreva et al. 2018b). This stage appears to be temporary, lasting less than 24 hours, upon which reversion occurs to the miniaturized trophic stage.

Under nutrient deprivation, the trophic stage of *Metadiplonema* differentiates into a smaller oval swimming stage with thickened flagella (Fig. 6C), which implies the presence of PFR, although this stage has not been studied at the ultrastructural level. Since a transient sessile stage has not been described in this genus, there might be a gradual transition from the trophic to the swimming stage. Among diplonemids that exhibit differentiation into several life stages, *Metadiplonema* is the only genus that contains extrusomes in the trophic stage (Nerad 1990; Schuster et al. 1968).

Members of the genus *Paradiplonema* are capable of swimming, although in the trophic stage this swimming does not involve the 'spinning lasso' pattern of the anterior flagellum typical for *Diplonema*, *Metadiplonema*, *Rhynchopus* and hemistasiids. Instead, the flagella bend in a manner that still enables rotational swimming (Fig. 6D). Elongated trophic cells will gradually grow more compact and

develop a diamond-like shape as nutrients grow scarce, before entering a rounded mucilage-enwrapped 'cyst-like' stage, which unlike *Diplonema* (see above) lacks the PFR as well as extrusomes and furthermore does not develop into the swimming stage (Nerad 1990; Porter 1973). However, their resistance to unfavorable environmental conditions and metabolic activity have never been evaluated. Hemistasiids, which swim under nutrient-rich conditions, such as *N. karyoxenos*, *Hemistasia phaecysticola* and *A. motanka*, can also take on the characteristic appearance of a sessile stage, similar to that of *Paradiplonema* (Fig. 6F) (Prokopchuk et al. 2019), with cultures typically containing both swimming and sessile cells. Other diplonemids do not exhibit discernible life stages, and display gliding (*Flectonema*), swimming (*Lacrimia*), immobile floundering (*Sulcionema*), or a combination thereof (Fig. 6E). Interestingly, the presence of PFR does not directly correlate with the swimming performance of diplonemids. Indeed, *P. papillatum*, which does not build a PFR, is capable of slow oscillating swimming similar to *Lacrimia* spp., which have long PFR-carrying flagella. Meanwhile, swimming has not been reported in the PFR-bearing *Flectonema* and *Sulcionema* spp. (Tashyreva et al. 2018a).

The morphological features of life stages offer clues to their nutritional modes. Swimming behavior likely constitutes a search for prey or new nutrient sources, whereas stages with limited movement are rather destined to stationary behaviors such as feeding and multiplication. Although in eukaryotic cells extrusomes have a range of functions, their positioning at the anterior of the diplonemid cell, adjacent to the FP, suggest offensive capabilities of predation or penetration into a host cell, although direct evidence for this is not yet available (Hausmann 1978). While some species permanently bear extrusomes, others such as *N. karyoxenos*, *D. japonicum* and *D. aggregatum* develop them only under nutrient-deprived conditions, further suggesting their use in nutrient acquisition.

Euglenozoans which form morphologically distinct stages in the course of their life cycle have been strongly associated with parasitism (Gibson 2017; Nerad 1990). Whether this is also the case in diplonemids remains unclear, since we are still unable to distinguish among parasitic, commensal and predatory behaviours (also see below). In any case, the temporary nature of swimming in both *D. japonicum* and *D. aggregatum* argues against the idea of viable predatory activity in this stage, rather suggesting a behaviour seeking a steady nutrient supply from a new host or source, upon which cells may return to the trophic mode.

Lifestyles and Feeding Strategies

All surveyed diplonemids are heterotrophs, with no photosynthetic organelles observed. The first-ever described *Diplonema* species, *D. breviciliata*, was suggested at the time to be a saprotroph (Griessmann 1914), and cultured diplonemids likely employ osmotrophy when cultivated in nutrient-rich artificial media. However, several species have recently been shown to be able to switch from osmotrophy to pure phagotrophy (Prokopchuk et al. 2022).

Feeding behavior has been most studied in hemistasiids, which were recognized as omnivorous predators. In addition to phagocytosis of whole prey cells, they are capable of entering other, usually much larger organisms, and consuming them from within. They have been reported to feed on a colonial haptophyte (Elbrächter et al. 1996; Scherffel 1900), diatoms (Elbrächter et al. 1996; Yabuki and Tame 2015), euglenids (Brandt née Tong and Sleigh 2000), dinoflagellates (Elbrächter et al. 1996), cryptophytes and chrysophytes (Brandt née Tong and Sleigh 2000) and copepods, as well as dead ciliates (Elbrächter et al. 1996). High abundances of *Hemistasia* sp. were noticed in plankton with blooming euglenids or haptophytes (Brandt née Tong and Sleigh 2000). However, feeding on live bacterial prey has not been observed.

Among Diplonemidae, feeding experiments have shown that *Rhynchopus euleeides* and *R. humris* are able to ingest bacteria (Prokopchuk et al. 2022; Roy et al. 2007). Moreover, the latter species has been shown to feed on dead microalgae, while *D. japonicum* was observed to feed on various types of nutrient sources, such as heat-killed bacteria, as well as living and dead microalgae (Prokopchuk et al. 2022). *Rhynchopus coscinodiscivorus* was observed to enter large diatoms, slowly consuming their cytoplasm and multiplying beneath their cell wall (Schnepf 1994). Other *Rhynchopus* spp. were reported in association with marine animals as parasites or commensals, as in the case of a lobster infected with a parasitic dinoflagellate *Hematodinium* sp., where diplonemids were observed in blood and on the gills (von der Heyden et al. 2004). Similarly, diplonemids were a part of a large

microbial community on the gills of a marine crab (Bodammer and Sawyer 1981) or were directly implicated with pathogenesis observed in cultured marine clams (Kent et al. 1987). Several Diplonemidae have been observed in association with aquatic plants. While *P. papillatum* was originally isolated from drifting marine eelgrass (Porter 1973), "*Diplonema*" *metabolicum* was found on tropical seagrass (Larsen and Patterson 1990). In neither case, however, was the diplonemid recorded within the plant tissue. By contrast, a species similar to *D. ambulator* was found within the cytoplasm of leaf cells of the freshwater plant *Cryptocoryne* shortly after the degenerative stages of '*Cryptocoryne* disease' occurred (Triemer and Ott 1990).

Although metabarcoding studies uncovered some hints about eupelagonemid ecology (see below), their role in planktonic communities remains mostly a mystery. For instance, six of 100 most abundant eupelagonemid operational taxonomic units (OTUs) were found predominantly in the meso-plankton fraction (180–2,000 μm), suggesting symbiotic or parasitic associations with large protists or small metazoans (Flegontova et al. 2016). Numerous abundant eupelagonemid OTUs were present primarily in the mesopelagic zone, in size fractions below 20 μm, with a positive correlation of abundances reported for selected eupelagonemid OTUs and Syndiniales or bacteria (Flegontova et al. 2016; Lima-Mendez et al. 2015). An analysis of V9 18S rRNA metabarcoding data showed that eupelagonemids prefer tropical regions and nutrient-rich conditions that follow algal blooms and avoid high oxygen concentrations (common at polar latitudes), high salinity, and high densities of algae during blooming periods (Flegontova et al. 2020). Based on these observations, it was hypothesized that a majority of eupelagonemids are not predators or symbionts of phytoplankton (Flegontova et al. 2020). However, microscopic evidence and single-cell genomic sequences suggest that at least some eupelagonemids prey upon phytoplankton, namely prasinophytes and haptophytes (Gawryluk et al. 2016).

Diversity and Ecology

Most microscopy observations of diplonemids are from marine environments, with almost all cultivated Diplonemidae species isolated from marine samples or aquaria (Nerad 1990; Porter 1973; Schuster et al. 1968; Tashyreva et al. 2018a). Although *Rhynchopus* was originally described from a freshwater sample (Skuja 1948), subsequent observations and isolations came from marine material (Nerad 1990; Schnepf 1994; Tashyreva et al. 2018a), or in one case, hypersaline samples (Ruinen 1938; identified as '*Menoidium astasia*'). Hemistasiidae appear to be marine (Griessmann 1914; Prokopchuk et al. 2019; Scherffel 1900), although they were also reported from brackish water (Elbrächter et al. 1996). The few observations of Eupelagonemidae that are reported as such are all marine cells (Gawryluk et al. 2016). Further, *Pronoctiluca*, which is morphologically very similar to some eupelagonemids despite being identified as an aberrant dinoflagellate, is also marine (Gómez 2013). The pattern of broader diversity and abundance of diplonemids in marine habitats, with only Diplonemidae being found in freshwater samples, is strongly supported and extended by environmental sequencing data (see below).

Members of Hemistasiidae were first described from the North Sea (Scherffel 1900). Their apparent worldwide distribution in coastal and open-ocean marine plankton, from the Arctic to Antarctic waters, was later recognized (Elbrächter et al. 1996). Even though all recently described Diplonemidae and Hemistasiidae species were isolated from a single site (Tokyo Bay, Japan), this is surely the result of a focused sampling effort, rather than other factors. Several diplonemids have been recorded in different countries, from coastal marine plankton and an aquarium (Larsen and Patterson 1990; Nerad 1990; Prokopchuk et al. 2019; Tashyreva et al. 2018a; Triemer and Ott 1990).

The extent of diplonemid diversity and potential ecological importance in marine systems became obvious only with the advent of environmental sequencing. An early study based on low-throughput methods revealed ~100 unique diplonemid 18S rRNA sequences in diverse planktonic samples, at varying depths (5 to 3,000 m depth, with most samples from the Atlantic Ocean and the Marmara Sea), which indicated high abundance and molecular diversity of Eupelagonemidae in marine plankton compared to Diplonemidae and Hemistasiidae (Lara et al. 2009). In subsequent high throughput metabarcoding studies relying on the hypervariable V9 region of the 18S rRNA gene (~130 nt long), diplonemids emerged as a prominent group in non-photic marine plankton and benthos, with abundance and diversity on par with major oceanic groups, such as metazoans, stramenopiles, dinoflagellates, and rhizarians (Cordier et al. 2022; Flegontova et al.

2016, 2020; Schoenle et al. 2021; de Vargas et al. 2015). A very high abundance of diplonemids in the bathypelagic zone (11% of eukaryotes) was also demonstrated using a metagenomic approach (Pernice et al. 2016) and clone-based environmental sequencing (Countway et al. 2007; López-García et al. 2007; Sauvadet et al. 2010).

By contrast, diplonemids are generally overlooked in V4 18S rRNA-based metabarcoding studies (Massana et al. 2015; Pernice et al. 2016) because the length of their V4 region exceeds 500 nt, making them technically unsuitable targets for high-throughput amplicon sequencing (Flegontova et al. 2016). High abundance of eupelagonemids was also not confirmed independently through the use of fluorescent in situ hybridization (FISH) with a diplonemid-specific probe (Morgan-Smith et al. 2013). In a FISH-based study of planktonic samples from the tropical Atlantic Ocean (100 to 7,000 m depth), the relative abundance of diplonemids and several other heterotrophic protist clades ranged between 1% and 3% of eukaryotic cells (Morgan-Smith et al. 2013).

The current absolute diversity of marine planktonic diplonemids in large V9 metabarcoding datasets stands at approximately 67,000 OTUs, which surpasses that of metazoans, stramenopiles, dinoflagellates, and rhizarians (Flegontova et al. 2020). However, the 100 most abundant OTUs account for 92.6% of all diplonemid reads, suggesting that a large majority of diplonemid OTUs have extremely low abundance (Flegontova et al. 2016). This predominance of just a few abundant OTUs is not a unique feature of these flagellates. Similar but less extreme patterns are observed in diatoms, pelagophytes, dinoflagellates, and some other protists (Keeling and del Campo 2017). Marine planktonic eupelagonemids account for >97% of total diplonemid OTUs and reads, with the other three clades (Diplonemidae, Hemistasiidae, and DSPD II) each accounting for about 1% or less (Flegontova et al. 2016, 2020). These proportions are also reflected in the 100 most abundant diplonemid OTUs, 97 of which belong to eupelagonemids, with just one OTU belonging to each of the other diplonemid clades (Flegontova et al. 2016).

An early study by Lara et al. (2009) reported that eupelagonemids (or, strictly speaking, their molecular signatures) are much more abundant in the meso- and bathypelagic layers than at the surface of the ocean. Other studies relying on much larger and geographically wider datasets have validated these observations. Indeed, the great majority of Eupelagonemidae OTUs (78 out of 97) and the most abundant DSPD II OTU occurs predominantly in the mesopelagic zone, whereas the most abundant OTUs of Diplonemidae and Hemistasiidae, along with 19 out of 97 most abundant Eupelagonemidae OTUs, occur mostly in the surface zone (Flegontova et al. 2016). It was also confirmed that the relative abundance of eupelagonemids increases with depth, reaches 14% on average in the mesopelagic zone versus 1% in the photic zone (Flegontova et al. 2016, 2020), and 5% in marine benthos (Schoenle et al. 2021). Both eupelagonemid diversity and relative abundance peak at around 750 to 1,000 m and then drop at greater depths (Flegontova et al. 2020). In early low-throughtput studies, eupelagonemids also appear to be a ubiquitous and abundant (up to 25% of eukaryotic sequences) component of deep marine plankton (Countway et al. 2007; López-García et al. 2007; Sauvadet et al. 2010). They were reported in the plankton at very large depths of up to 5,600 m (Scheckenbach et al. 2010) and 6,000 m (Eloe et al. 2011). In smaller V9 metabarcoding datasets of deep marine benthos (3 bathyal, 15 abyssal and 2 hadal worldwide locations), diplonemids appear as the most diverse eukaryotic group, with approximately 13,000 OTUs (Schoenle et al. 2021).

Eupelagonemid community composition depends on depth, geography, oxygen concentration, salinity, temperature, and on environmental variables that typically reflect the abundance of algae and nutrients (Flegontova et al. 2016, 2020). Some eupelagonemid OTUs occurred in geographically distant environments and in very different water masses, and a high diversity of OTUs was found within a single sample (Lara et al. 2009). A substantial decrease in eupelagonemid richness and relative abundance was observed in regions of high oxygen concentrations. In contrast, eupelagonemid richness remains very high in nearly anoxic samples (oxygen concentration from 0 to 1 mg/l) (Flegontova et al. 2020).

Recently, several studies focused on freshwater diplonemids using metabarcoding, shotgun metagenomics and catalyzed reporter deposition-FISH. In contrast to marine diplonemids, freshwater diplonemids were detected in low abundance (less than 1% of eukaryotes) in the plankton of several lakes in Japan, the Czech Republic, and Switzerland (Mukherjee et al. 2020), and in the plankton and sediments of Lake Baikal (David et al. 2021;

Reboul et al. 2021; Yi et al. 2017). Their 18S rRNA sequences fall within the Diplonemidae clade (David et al. 2021; Mukherjee et al. 2020), corresponding to earlier light microscopy studies in which only this diplonemid group was observed in freshwater habitats (Skuja 1948; Triemer and Ott 1990).

Genomics

A high-quality nuclear genome for diplonemids is yet to be assembled, although several genome projects are currently underway. Existing estimates of the size of their nuclear genome, based on single-cell sequencing data, vary from ~16 to 309 Mb (Gawryluk et al. 2016). The genome of an axenically cultured *P. papillatum* was sequenced using short Illumina reads, resulting in a highly fragmented assembly totalling ~177 Mb (Morales et al. 2016). The genomes of diplonemids are rich in non-canonical introns lacking conventional GT-AG splice sites (Gawryluk et al. 2016). Genes are transcribed in a polycistronic manner, where multiple genes are encompassed within a transcription unit, and must be separated *via* splicing. Nuclear gene expression in diplonemids apparently requires both *cis*- and *trans*-splicing of mRNAs. While the former process involves the removal of introns typical of eukaryotes, the latter case involves a more rarely encountered attachment of a spliced leader RNA gene sequence to the 5′-end of all nucleus-encoded transcripts (Butenko et al. 2021). The relatively large genome sizes and richness in long repeats hamper obtaining a chromosome-level assembly for diplonemids, making the application of long read technologies indispensable.

The coding capacity of diplonemid genomes, estimated from the transcriptomic data, varies from ~37,000 to ~ 52,000 genes in *R. humris* and *H. phaeocysticola*, respectively (Butenko et al. 2020). The analysis of metabolic pathways based on transcriptome assemblies hints that diplonemids are highly metabolically versatile, with the number of enzymes encoded in their genomes being comparable or even surpassing that of photosynthetic euglenids (Butenko et al. 2020). Diplonemids analyzed in this respect are able to synthetize all nucleotides, 20 amino acids, and vitamins, with fatty acids synthesized using cytosolic fatty acid synthase (FAS) I. Although the majority of FAS II enzymes were identified, the critical enzyme responsible for the transfer of malonyl to acyl carrier protein (ACP) in the initial step (malonyl-coenzyme A-ACP transacylase) was missing in all transcriptomes (Butenko et al. 2020; Škodová-Sveráková et al. 2021). Searches in the available transcriptome assemblies for the elements of several fundamental cellular machines, such as the replication origin recognition complex and the kinetochore, suggests their divergence beyond recognition or their replacement by novel components (Butenko et al. 2020).

The mitochondrial genomes of diplonemids are especially interesting, particularly from an evolutionary perspective. Their mitochondrion harbors the highest quantity of mitochondrial DNA (mtDNA) documented for an organelle (Lukeš et al. 2018). The mtDNA includes typical mitochondrial genes for several subunits of the electron transport chain (ETC) complexes (Faktorová et al. 2018), namely one ATP synthase subunit (*atp6*), cytochrome *b* (*cob*), three subunits of cytochrome *c* oxidase (*cox1*, *cox2*, and *cox3*) and 10 subunits of NADH dehydrogenase (*nad1*, *nad2*, *nad3*, *nad4*, *nad4L*, *nad5*, *nad6*, *nad7*, *nad8*, and *nad9*), as well as two additional proteins (*y4* and *y7*). The function of *y7* is unknown, but *y4* may represent a divergent mitochondrial ribosomal protein or subunit of an ETC complex (Kaur et al. 2020; Valach et al. 2018). Diplonemids do not encode any tRNA genes in their mitochondrial genomes, and their small and large subunits of mitoribosomal RNAs (*rns* and *rnl*) are the shortest of all those currently known (Valach et al. 2017). Their mitochondrial genes utilize a non-standard genetic code, with TGA encoding tryptophan instead of denoting a translational stop, similar to other euglenozoans (Záhonová et al. 2021).

The expression of the mtDNA in diplonemids is quite extraordinary in terms of its complexity (Burger and Valach 2018; Faktorová et al. 2018; Valach et al. 2017). Genes are split into smaller fragments (modules) that are encoded on separate circular non-catenated chromosomes. The number of modules and chromosomes is taxon-dependent, with twice as many modules seen in Hemistasiidae (170 modules on 163 chromosomes in *N. karyoxenos*) than in Diplonemidae (80 modules on 30 chromosomes in *D. japonicum*) (Kaur et al. 2020). Modules are enclosed within a unique region (cassette), which is surrounded by a class-specific repetitive sequence (constant region). Cassettes contain one or several modules that may overlap or be embedded within each other. Possessing 15 overlapping or embedded modules, *A. motanka* is the record holder in this respect (Kaur et al. 2020). Modules are transcribed separately with flanking regions endonucleolytically removed and module ends

exonucleolytically trimmed. The mono-module transcripts are *trans*-spliced together as soon as one of the module termini is end-processed. *Trans*-splicing starts with any two processed modules, joining consecutive modules without any preferred order. The *trans*-splicing mechanism remains unknown, although it is well-established that this is not catalyzed by spliceosomes, group I, or group II introns (Burger and Valach 2018; Kiethega et al. 2013).

Another level of complexity is added at the post-transcriptional level, as mitochondrial transcripts undergo massive RNA editing of three different types (Kaur et al. 2020; Kiethega et al. 2013; Moreira et al. 2016; Valach et al. 2017). Modules are subject to uridine and adenine additions (U- and A-appendage) at their 3′ ends. Moreover, numerous adenosines and cytidines are deaminated to inosines (A-to-I) and uridines (C-to-U), respectively, and in a few instances in hemistasiids, guanosines are changed to adenosines (G-to-A). In 17 mitochondrial genes of *N. karyoxenos* more than 1,000 C-to-U and A-to-I substitutions, 14 G-to-A changes, and 94 U+A-appended tracts altogether account for 12.2% editing density, qualifying *N. karyoxenos* as an organism with the most heavily edited organellar transcriptome (Kaur et al. 2020). It appears that mitochondrial transcripts of eupelagonemids undergo the same processes, i.e., *trans*-splicing and post-transcriptional RNA editing (Kaur et al. 2020), however, sequence data from more eupelagonemids and species of the DSPD II clade is needed to confirm whether these unique characteristics are a unifying feature for all diplonemids.

Metabolism

The metabolism of *P. papillatum* has been examined using a combination of transcriptomic, pro-

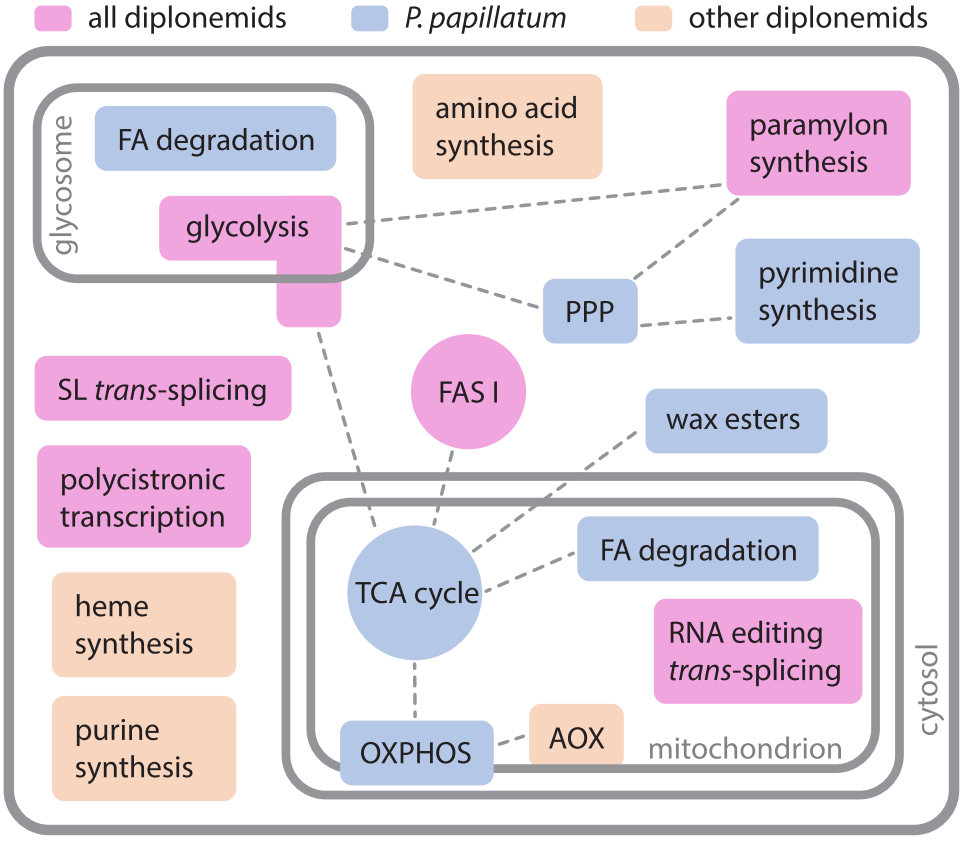

Figure. 7. Metabolic pathways identified in the transcriptomes of diplonemids. Pathways analyzed only in *Paradiplonema papillatum* are in blue, in several diplonemids (*Rhynchopus humris*, *Sulcionema specki*, and *Hemistasia phaeocysticola*) in orange, and in all diplonemids in pink. Paramylon synthesis, and mitochondrial RNA editing and *trans*-splicing were studied in *P. papillatum*, *D. japonicum*, *R. humris*, *L. lanifica*, *S. specki*, *A. motanka*, and *N. karyoxenos*. All other pink boxes represent studies in *P. papillatum*, *R. humris*, *S. specki*, and *H. phaeocysticola*, but based on their presence in different groups, we predict their universal occurrence in diplonemids.

teomic and metabolomic approaches supplemented with biochemical experiments (Fig. 7) (Škodová-Sveráková et al. 2021). Thus far, it is the only diplonemid investigated in any depth at a metabolic level. *P. papillatum* possesses the full enzymatic machinery for fundamental metabolic pathways such as glycolysis, gluconeogenesis, the pentose phosphate pathway (PPP), the tricarboxylic acid (TCA) cycle, synthesis and β-oxidation of fatty acids (FA), and oxidative phosphorylation (OXPHOS), altogether reflecting the capability to generate ATP *via* substrate-level phosphorylation and OXPHOS (Škodová-Sveráková et al. 2021).

An early study showed that gluconeogenesis dominates over glycolysis (Morales et al. 2016). The glucose anabolic pathway was reconstructed up to glucose synthesis (Škodová-Sveráková et al. 2021), and although the sequence annotated as glucose-6-phosphatase (GPase) belongs to a broader protein family of GPases, it lacks crucial protein domains facilitating its functionality. Therefore, glycolysis may proceed only up to the generation of glucose-6-phosphate (G6P), which can be directly employed by the PPP (or vice versa) or condensed into the β-1,3 glucan (paramylon), which is otherwise characteristic of many euglenids. The presence of paramylon in *P. papillatum* was demonstrated through the recovery of glucose monomers from an acid-digested polymer, as well as by antibodies against 1,3-β-glucan linkages (Škodová-Sveráková et al. 2020). All analyzed transcriptomes (*P. papillatum*, *D. japonicum*, *R. humris*, *L. lanifica*, *S. specki*, *N. karyoxenos*, and *A. motanka*) additionally contain transcripts of the glucan synthase inferred to be responsible for paramylon synthesis in *P. papillatum* (Škodová-Sveráková et al. 2020), suggesting a capacity for other species to synthesize this macromolecule as well. However, the conditions and purpose of paramylon synthesis in diplonemids seem to differ from that in *Euglena gracilis*. While paramylon accumulates in *E. gracilis* under excess nutrients (Barsanti et al. 2001), *P. papillatum* amassed it under nutrient-poor conditions (Škodová-Sveráková et al. 2020). Its possible functions include a role in the development of resting cysts (Ellegaard and Ribeiro 2017) or increasing cell density, enabling organisms to sink into deeper ocean strata where nutrient availability is potentially more favorable (Jensen et al. 2020).

In *E. gracilis*, paramylon breakdown is linked to an adaption to anaerobiosis and subsequently to wax ester synthesis (Nakazawa et al. 2018). Enzymes of wax ester synthesis were similarly identified in the transcriptome of *P. papillatum*, together with other anaerobic enzymes, such as pyruvate: NADP+ oxidoreductase (PNO), fumarate reductase, enoyl-coenzyme A (CoA) reductase, lactate dehydrogenase, and opine dehydrogenase (Škodová-Sveráková et al. 2021). Their functionality requires exploration, however: even when *P. papillatum* was deprived of oxygen, cells decreased their metabolic and division rates, rather than upregulating enzymes facilitating survival in anaerobic environments (Škodová-Sveráková et al. 2021).

The PPP is the major consumer of G6P; hence it is tightly connected to gluconeogenesis in *P. papillatum*, which does not uptake glucose directly from its environment (Morales et al. 2016). The PPP's primary role is to synthesize NADPH as an electron carrier for the maintenance of redox homeostasis and reductive biosynthesis, such as the FA synthesis. Enzymes of *P. papillatum* PPP were all localized into the cytosol, except for ribulose-5-phosphate epimerase which harbors a peroxisomal (i.e. glycosomal) targeting signal (PTS) (Škodová-Sveráková et al. 2021). However, in the kinetoplastid *Trypanosoma brucei,* many of these enzymes without a recognizable PTS are found both in the glycosomes and the cytosol (Heise and Opperdoes 1999; Kovářová and Barrett 2016). It is possible that cryptic (PTS-independent) targeting to the glycosome is a feature of both kinetoplastids and diplonemids.

The inferred functioning of the TCA cycle in *P. papillatum* is somewhat complicated due to the presence of 2-oxoglutarate dehydrogenase (OGDH) and succinyl-CoA synthetase, in addition to their alternative enzymes, 2-oxoglutarate decarboxylase (OGDC) and succinate-semialdehyde dehydrogenase (SSDH), respectively (Škodová-Sveráková et al. 2021). Both pairs of enzymes catalyze the conversion of 2-oxoglutarate into succinate. In the classical TCA cycle, this leads to the production of NADH and ATP, while in the alternative shunt no ATP (or GTP) is formed, and NADPH is produced instead of NADH. Since OGDC catalyzes an irreversible decarboxylation reaction, the cycle runs only in one direction, while OGDH catalyzes a reversible reaction, potentially enabling catabolic and anabolic outputs. The operating conditions of each branch remain unknown, since *P. papillatum* represents the first organism where both branches were identified simultaneously. The high accumulation of OGDC when oxygen is available (Škodová-Sverá

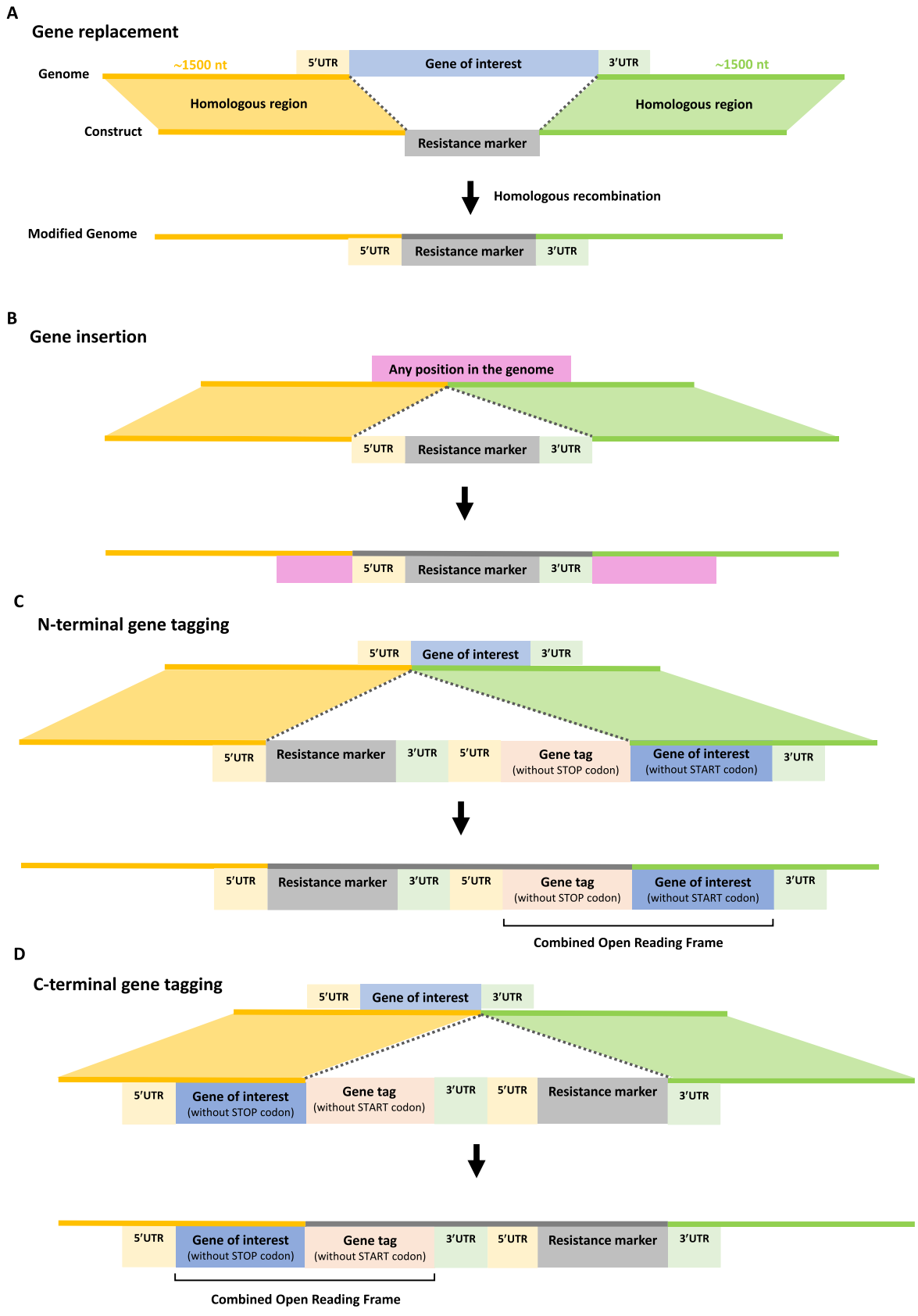
A
Gene replacement
Genome
~1500 nt
5′UTR
Gene of interest
3′UTR
~1500 nt
Homologous region
Homologous region
Construct
Resistance marker
Homologous recombination
Modified Genome
5′UTR
Resistance marker
3′UTR
B
Gene insertion
Any position in the genome
5′UTR
Resistance marker
3′UTR
5′UTR
Resistance marker
3′UTR
C
N-terminal gene tagging
5′UTR
Gene of interest
3′UTR
5′UTR
Resistance marker
3′UTR
5′UTR
Gene tag
(without STOP codon)
Gene of interest
(without START codon)
3′UTR
5′UTR
Resistance marker
3′UTR
5′UTR
Gene tag
(without STOP codon)
Gene of interest
(without START codon)
3′UTR
Combined Open Reading Frame
D
C-terminal gene tagging
5′UTR
Gene of interest
3′UTR
5′UTR
Gene of interest
(without STOP codon)
Gene tag
(without START codon)
3′UTR
5′UTR
Resistance marker
3′UTR
5′UTR
Gene of interest
(without STOP codon)
Gene tag
(without START codon)
3′UTR
5′UTR
Resistance marker
3′UTR
Combined Open Reading Frame

ková et al. 2021), however, suggests its involvement in aerobic metabolism, as described for *E. gracilis* where OGDC together with SSDH represent the sole pathways of the TCA cycle (Nakazawa et al. 2017). In *E. gracilis* the TCA cycle is fueled by acetyl-CoA, as a product of pyruvate metabolism, which enters the cycle *via* condensation with oxaloacetate to produce citrate. Due to the preference of *P. papillatum* for gluconeogenesis, pyruvate most likely originates from amino acid metabolism. Some amino acids enter the TCA cycle in an intermediate step. For example, proline is converted by proline dehydrogenase into 2-oxoglutarate and undergoes extensive oxidation further in the TCA cycle (Škodová-Sveráková et al. 2021). Succinate dehydrogenase connects the central metabolism with the electron transport chain and OXPHOS. *P. papillatum* takes advantage of oxygen-rich metabolism and involves all respiratory complexes, as well as alternative enzymes to transfer electrons from reduced equivalents to oxygen. The engagement of PNO for anaerobic oxidation of pyruvate is therefore worth a targeted study. Since some diplonemid OTUs are abundant in anoxic regions of the deep ocean (Flegontova et al. 2020), it is likely that the anaerobic enzymes identified in *P. papillatum* are common for this group of marine protists.

Genetic Manipulation

The recently recognized diversity, abundance, and ecological significance of diplonemids (see above) has brought to the fore the need to develop at least one species into a genetically tractable organism, to better understand their biology, interactions, ecology, and function of individual proteins. Since a representative of the most species-rich eupelagonemid clade has not yet been introduced into culture, a transformation system has been developed for *P. papillatum*, which can be cultivated axenically, reaches high cell density and can be easily cryopreserved.

The identification of selection markers along with suitable transformation conditions allowed the preparation of constructs that stably integrate into the genome and are efficiently transcribed. Moreover, their transcripts are processed and translated on cytosolic ribosomes. The construct design, along with transformation protocol, was inspired by the extensive knowledge available for *T. brucei* (Dean et al. 2015). Combined, we were able to show that both the fluorescence gene and the resistance markers of the electroporated constructs were transcribed and that the spliced leader RNA was *trans*-spliced to the 5´ ends of nuclear-encoded transcripts. Moreover, the resistance markers were translated into proteins, thus demonstrating that *P. papillatum* can be stably transformed and now represents a genetically tractable species (Faktorová et al. 2020a; Kaur et al. 2018). An important limit of both studies, however, was the failure of the constructs to integrate into the target genomic locus. Initially, 100 nt-long homologous regions were used, which were later increased to 500 nt (Kaur et al. 2018). Despite this, both constructs were integrated randomly across the genome, although homologous recombination is likely functioning in *P. papillatum*.

A hypothesis that *P. papillatum* uses microhomologies or non-homologous end-joining pathway as the main DNA repair and/or recombination pathway was tested by blocking both pathways, yet targeting of the construct to the expected position was not achieved. Eventually, targeted integration by homologous recombination was achieved *via* fusion PCR-based method by extending the 5´and 3´ homologous flanking regions to 1,000–2,000 nt. The available protocol allows robust gene replacement and tagging (Faktorová et al. 2020b). Thus, *P. papillatum* has expanded the still rather short list of genetic models among marine microeukaryotes (Faktorová et al. 2020a).

Finally, a modular protein-A tag-bearing plasmid has been designed that serves as a universal template for the C- and N- terminal gene tagging, which represent a key prerequisite for further functional analyses and identification of protein complexes. The construct was inserted *via* homologous recombination into a repetitive intergenic region (Faktorová et al. 2020b). Since a robust, reproducible transfection protocol that allows gene knock-out and knock-in manipulations, as well as

Figure 8. Currently available tools for genetic modifications of *P. papillatum.* The situation in the genome (top) is shown together with the schemes of the individual constructs (bottom) designed for genome modifications based on homologous recombination: **A.** Gene replacement, **B.** Gene insertion, **C.** N-terminal gene tagging or **D.** C-terminal gene tagging. The individual elements are shown in colors, increased length of the homologous regions (N-terminal in orange, C-terminal in green) to 1,000 to 2,000 nt enables targeted integration of the constructs.

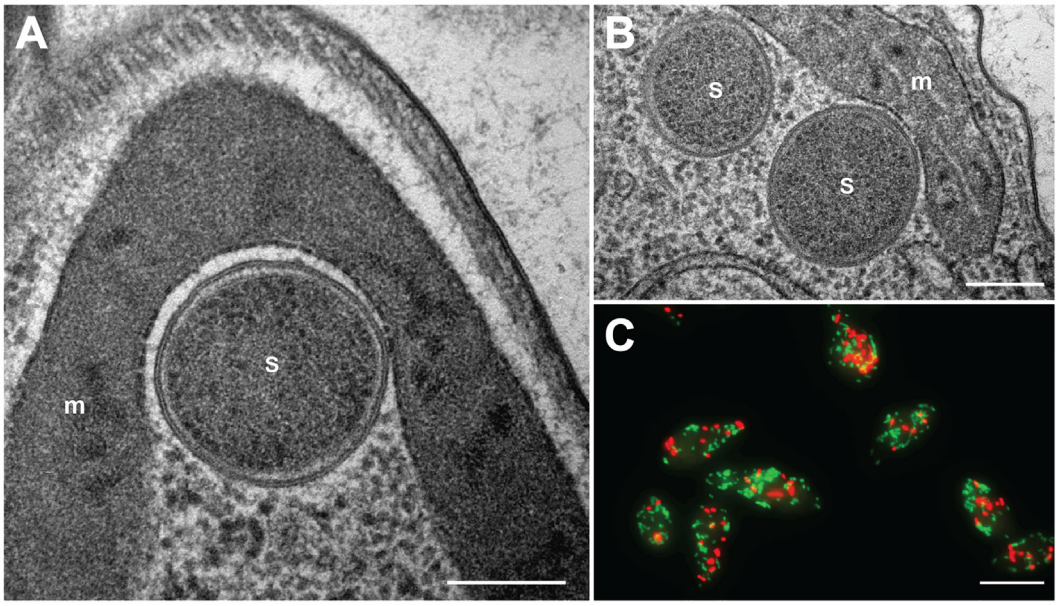

Figure 9. Localization of bacterial endosymbionts in diplonemids. **A-B.** Transmission electron microscopy of bacterial endosymbionts (*s*) associated with *Diplonema japonicum* mitochondria (*m*). **C.** Fluorescence *in situ* hybridization of the bacterial endosymbionts, *Cytomitobacter primus* (red) and *Nesciobacter abundans* (green), in *Diplonema japonicum*. Scale bars: 200 nm (A,B), 10 μm (C).

the C- and N-terminal gene tagging has now been established in *P. papillatum* (Fig. 8), the same procedure can be applied to other diplonemid species available in culture, which may be of greater ecologically relevance. Another promising extension of the above-mentioned techniques would be CRISPR/Cas9 technology and RNA interference, tools extensively used in *T. brucei* and other trypanosomatids (Matthews 2015).

Endosymbionts

Diplonemids harbor several different bacterial endosymbionts from the alphaproteobacterial orders *Holosporales* and *Rickettsiales* (George et al. 2020; Prokopchuk et al. 2019; Tashyreva et al. 2018b). Both orders are made up of intracellular bacteria found in diverse eukaryotic hosts, ranging from single-celled algae to animals (Husnik et al. 2021). The endosymbionts have been described from two families of diplonemids where they reside in the host's cytoplasm and/or nucleus (Prokopchuk et al. 2019). The endosymbionts also interact closely with the mitochondrion (Fig. 9), and in some cases, the bacterial cells are almost entirely surrounded by this organelle (Tashyreva et al. 2018b). *Diplonema japonicum* harbors two different *Holosporales* endosymbionts, *Nesciobacter abundans* and *Cytomitobacter primus*, with *N. abundans* having higher abundance than *C. primus* during all host life stages (Fig. 9C) (George et al. 2020). Another species of *Cytomitobacter*, *C. indipagum*, is found in *D. aggregatum*, while *N. karyoxenos* contains a *Rickettsiales* endosymbiont, *Sneabacter namystus* (Prokopchuk et al. 2019).

All diplonemid endosymbionts sequenced to date carry highly reduced genomes, and the smallest *Holosporales* endosymbiont genome (*N. abundans*) contains only 505 protein-coding genes (616 kb), most of which have unknown functions (George et al. 2020). These endosymbionts have converged on a similar small genome size (605 to 632 kb) and genome content, despite belonging to different bacterial orders. Essential genetic machineries (e.g., replication, transcription, and translation) have been retained, but the endosymbionts' metabolic potential is severely reduced, as they lack glycolysis, TCA cycle and OXPHOS. This reduced metabolic potential is compensated by several metabolite transports such as ATP/ADP translocases, which allow the import of ATP or ADP from the diplonemid host, offering an explanation for the endosymbionts' close association with mitochondria. The reduction of carbon metabolism is common in *Rickettsiales* and *Holosporales* endosymbionts, but the severity of

the reduction documented in the diplonemid endosymbionts is rare (e.g., complete loss of oxidative phosphorylation) (George et al. 2020; Husnik et al. 2021). Therefore, host factors likely play a role in the convergence of the endosymbionts' reduced metabolism.

Despite their small genomes, the diplonemid endosymbionts possess multiple secretion systems, including a type VI secretion system (T6SS). T6SS are used for interspecific competition in free-living bacteria where the sharp, needle-like tip punctures a competitor's cell membrane and injects a toxin known as an effector protein (Steele et al. 2017). The endosymbionts encode a T6SS effector protein (VgrG1) as well as an immunity protein (YwqK), but the function of these endosymbiotic T6SSs remains unclear; they may help protect the host from invading bacteria or they may be modified for host interactions. The endosymbionts also harbor several proteins with leucine-rich repeats (LRRs), which are involved in eukaryotic protein-protein interactions (Kobe and Kajava 2001), and some bacterial endosymbionts use proteins with LRRs for eukaryotic cell invasion (Zhou and Chai 2008). Interestingly, several genes with LRRs are encoded next to the T6SS effector protein in the *Holosporales* endosymbiont genomes, suggesting that the endosymbiotic T6SSs are involved in symbiont-host interactions.

The potential functional role and stability of the symbioses are unknown. The bacterial endosymbionts of diplonemids are likely energy parasites, given their reduced metabolism and relatedness to other *Rickettsiales* and *Holosporales* parasites. However, this does not rule out beneficial functions, such as the possible defensive roles discussed above, which are difficult to study once the host is removed from the environment and established in culture. Alternatively, the endosymbionts may be commensals with little or no effect on their host. Whether or not the host relies on the endosymbionts or if transmission of the endosymbionts can occur between different diplonemid species remain open questions. Future studies will shed light on the evolution and ecology of these bacterial endosymbionts of microbial eukaryotes.

Conclusions and Future Perspectives

While diplonemids were neglected for nearly a century since their initial description, data collected within the last decade unambiguously document that these protists are neither obscure, nor mundane. Recent efforts have brought a multitude of species into culture, allowing comprehensive studies of their cell and molecular biology, as well as behavior. Based on their staggering amount and diversity, we propose that diplonemids fulfill a wide range of ecological roles, and these can now be studied. Multiple whole genome sequencing projects currently in progress point to a wealth of knowledge available on the horizon, which shall shed light on new aspects of the often baroque aspects of diplonemid molecular biology. The establishment of genetic tractability for *P. papillatum* will enable a range of functional studies and holds promise for genetic manipulations of other diplonemids. The newly available methodology shall attract an increasing number of researchers to these still enigmatic protists.

Declaration of Competing Interest

The authors declare that they have no known competing financial interests or personal relationships that could have appeared to influence the work reported in this paper.

Acknowledgements

We thank all members of the Lukeš lab, Paul A.M. Michels (University of Edinburgh), Fred Opperdoes (University of Louvain), Dave Speijer (University of Amsterdam), and Matus Valach and Gertraud Burger (University of Montreal) for discussions. This work was supported by grants from the Czech Science Foundation 18-23787S (to AH and GP), the ERC CZ LL1601 and the ERD project 16_019/0000759 (to JL), the Czech BioImaging grant LM2018129 (to DT), and the Gordon and Betty Moore Foundation (to PJK and JL).

Appendix A. Supplementary Data

Supplementary data to this article can be found online at https://doi.org/10.1016/j.protis.2022.125868.

References

Barsanti L, Vismara R, Passarelli V, Gualtieri P (2001) Paramylon (β-1,3-glucan) content in wild type and WZSL mutant of *Euglena gracilis*. Effects of growth conditions. J Appl Phycol **13**:59–65

Bodammer JE, Sawyer TK (1981) Aufwuchs protozoa and bacteria on the gills of the rock crab, *Cancer irroratus* Say: a survey by light and electron microscopy. J Protozool **28**:35–46

Boeuf D, Edwards BR, Eppley JM, Hu SK, Poff KE, Romano AE, Caron DA, Karl DM, DeLong EF (2019) Biological composition and microbial dynamics of sinking particulate organic matter at abyssal depths in the oligotrophic open ocean. Proc Natl Acad Sci USA **116**:11824–11832

Brandt née Tong SM, Sleigh MA (2000) The quantitative occurrence of different taxa of heterotrophic flagellates in Southampton water, U.K. Estuar Coast Shelf Sci **51**:91–102

Breglia SA, Slamovits CH, Leander BS (2007) Phylogeny of phagotrophic euglenids (Euglenozoa) as inferred from hsp90 gene sequences. J Eukaryot Microbiol **54**:86–92

Burger G, Valach M (2018) Perfection of eccentricity: mitochondrial genomes of diplonemids. IUBMB Life **70**:1197–1206

Busse I, Preisfeld A (2002) Phylogenetic position of *Rhynchopus* sp. and *Diplonema ambulator* as indicated by analyses of euglenozoan small subunit ribosomal DNA. Gene **284**:83–91

Butenko A, Hammond M, Field MC, Ginger ML, Yurchenko V, Lukeš J (2021) Reductionist pathways for parasitism in euglenozoans? Expanded datasets provide new insights. Trends Parasitol **37**:100–116

Butenko A, Opperdoes FR, Flegontova O, Horák A, Hampl V, Keeling P, Gawryluk RMR, Tikhonenkov D, Flegontov P, Lukeš J (2020) Evolution of metabolic capabilities and molecular features of diplonemids, kinetoplastids, and euglenids. BMC Biology **18**:23

Cavalier-Smith T (1993) Kingdom protozoa and its 18 phyla. Microbiol Rev **57**:953–994

Cavalier-Smith T (2016) Higher classification and phylogeny of Euglenozoa. Europ J Protistol **56**:250–276

Cordier T, Angeles IB, Henry N, Lejzerowicz F, Berney C, Morard R, Brandt A, Cambon-Bonavita M-A, Guidi L, Lombard F, Martinez Arbizo P, Massana R, Orejas C, Poulain J, Smith CR, Wincker P, Arnaud-Haond S, Gooday AJ, de Vargas C, Pawlowski J (2022) Patterns of eukaryotic diversity from the surface to the deep-ocean sediment. Sci Adv **8(5)**:eabj9309

Countway PD, Gast RJ, Dennett MR, Savai P, Rose JM, Caron DA (2007) Distinct protistan assemblages characterize the euphotic zone and deep sea (2500 m) of the western North Atlantic (Sargasso Sea and Gulf Stream). Environ Microbiol **9**:1219–1232

David GM, Moreira D, Reboul G, Annenkova NV, Galindo LJ, Bertolino P, López-Archilla AI, Jardillier L, López-García P (2021) Environmental drivers of plankton protist communities along latitudinal and vertical gradients in the oldest and deepest freshwater lake. Environ Microbiol **23**:1436–1451

de Vargas C, Audic S, Henry N, Decelle J, Mahé F, Logares R, Lara E, Berney C, Le Bescot N, Probert I, Carmichael M, Poulain J, Romac S, Colin S, Aury JM, Bittner L, Chaffron S, Dunthorn M, Engelen S, Flegontova O, Guidi L, Horák A, Jaillon O, Lima-Mendez G, Lukeš J, Malviya S, Morard R, Mulot M, Scalco E, Siano R, Vincent F, Zingone A, Dimier C, Picheral M, Searson S, Kandels-Lewis S, Tara Oceans Coordinators SG, Acinas SG, Bork P, Bowler C, Gorsky G, Grimsley N, Hingamp P, Iudicone D, Not F, Ogata H, Pesant S, Raes J, Sieracki ME, Speich S, Stemmann L, Sunagawa S, Weissenbach J, Wincker P, Karsenti E (2015) Ocean plankton. Eukaryotic plankton diversity in the sunlit ocean. Science **348**:1261605

Dean S, Sunter J, Wheeler RJ, Hodkinson I, Gluenz E, Gull K (2015) A toolkit enabling efficient, scalable and reproducible gene tagging in trypanosomatids. Open Biol **5**: 140197

Elbrächter M, Schnepf E, Balzer I (1996) *Hemistasia phaecysticola* (Scherffel) comb. nov., redescription of a free-living, marine, phagotrophic kinetoplastid flagellate. Arch Protistenkd **147**:125–136

Ellegaard M, Ribeiro S (2017) The long-term persistence of phytoplankton resting stages in aquatic 'seed banks'. Biol Rev Camb Philos Soc **93**:166–183

Eloe EA, Shulse CN, Fadrosh DW, Williamson SJ, Allen EE, Bartlett DH (2011) Compositional differences in particle-associated and free-living microbial assemblages from an extreme deep-ocean environment. Environ Microbiol Rep **3**:449–458

Faktorová D, Valach M, Kaur B, Burger G, Lukeš J (2018) Mitochondrial RNA Editing and Processing in Diplonemid Protists. In Cruz-Reyes J, Gray M (eds) RNA Metabolism in Mitochondria. Nucleic Acids and Molecular Biology; Springer, Cham, pp 145–176

Faktorová D, Kaur B, Valach M, Graf L, Benz C, Burger G, Lukeš J (2020) Targeted integration by homologous recombination enables in-situ tagging and replacement of genes in the marine microeukaryote *Diplonema papillatum*. Environ Microbiol **a22**:3660–3670

Faktorová D, Nisbet RER, Fernández Robledo JA, Casacuberta E, Sudek L, Allen AE, Ares Jr M, Aresté C, Balestreri C, Barbrook AC, Beardslee P, Bender S, Booth DS, Bouget FY, Bowler C, Breglia SA, Brownlee C, Burger G, Cerutti H, Cesaroni R, Chiurillo MA, Clemente T, Coles DB, Collier JL, Cooney EC, Coyne K, Docampo R, Dupont CL, Edgcomb V, Einarsson E, Elustondo PA, Federici F, Freire-Beneitez V, Freyria NJ, Fukuda K, García PA, Girguis PR, Gomaa F, Gornik SG, Guo J, Hampl V, Hanawa Y, Haro-Contreras ER, Hehenberger E, Highfield A, Hirakawa Y, Hopes A, Howe CJ, Hu I, Ibañez J, Irwin NAT, Ishii Y, Janowicz NE, Jones AC, Kachale A, Fujimura-Kamada K, Kaur B, Kaye JZ, Kazana E, Keeling PJ, King N, Klobutcher LA, Lander N, Lassadi I, Li Z, Lin S, Lozano JC, Luan F, Maruyama S, Matute T, Miceli C, Minagawa J, Moosburner M, Najle SR, Nanjappa D, Nimmo IC, Noble L, Novák Vanclová AMG, Nowacki M,

Nuñez M, Pain A, Piersanti A, Pucciarelli S, Pyrih J, Rest JS, Rius M, Robertson D, Ruaud A, Ruiz-Trillo I, Sigg MA, Silver PA, Slamovits CH, Jason Smith G, Sprecher BN, Stern R, Swart EC, Tsaousis AD, Tsypin L, Turkewitz A, Turnšek J, Valach M, Vergé V, von Dassow P, von der Haar T, Waller RF, Wang L, Wen X, Wheeler G, Woods A, Zhang H, Mock T, Worden AZ, Lukeš J (2020) Genetic tool development in marine protists: emerging model organisms for experimental cell biology. Nat Methods **b17**:481–494

Flegontova O, Flegontov P, Londoño PAC, Walczowski W, Šantić D, Edgcomb VP, Lukeš J, Horák A (2020) Environmental determinants of the distribution of planktonic diplonemids and kinetoplastids in the oceans. Environ Microbiol **22**:4014–4031

Flegontova O, Flegontov P, Malviya S, Audic S, Wincker P, de Vargas C, Bowler C, Lukeš J, Horák A (2016) Extreme diversity of diplonemid eukaryotes in the ocean. Curr Biol **26**:3060–3065

Gawryluk RMR, Del Campo J, Okamoto N, Strassert JFH, Lukeš J, Richards TA, Worden AZ, Santoro AE, Keeling PJ (2016) Morphological identification and single-cell genomics of marine diplonemids. Curr Biol **26**:3053–3059

George EE, Husnik F, Tashyreva D, Prokopchuk G, Horák A, Kwong WK, Lukeš J, Keeling PJ (2020) Highly reduced genomes of protist endosymbionts show evolutionary convergence. Curr Biol **30**:925–933.e3

Gibson W (2017) Kinetoplastea. In Archibald JM, Simpson AGB, Slamovits CH (eds) Handbook of the Protists. 2nd edn. Springer Cham, pp 1089–1138.

Gómez F (2013) Morphology and distribution of *Pronoctiluca* (Dinoflagellata, incertae sedis) in the Pacific Ocean. Acta Oceanol Sin **32**:71–76

Griessmann K (1914) Über marine Flagellaten. Arch Protistenkd **32**:1–78

Hausmann K (1978) Extrusive organelles in protists. Int Rev Cytol **52**:197–276

Heise N, Opperdoes FR (1999) Purification, localisation and characterisation of glucose-6-phosphate dehydrogenase of *Trypanosoma brucei*. Mol Biochem Parasitol **99**:21–32

Husnik F, Tashyreva D, Boscaro V, George EE, Lukeš J, Keeling PJ (2021) Bacterial and archaeal symbioses with protists. Curr Biol **31**:R862–R877

Jensen EL, Yangüez K, Carrière F, Gontero B (2020) Storage compound accumulation in diatoms as response to elevated CO_2 concentration. Biology **9**:5

Kaur B, Záhonová K, Valach M, Faktorová D, Prokopchuk G, Burger G, Lukeš J (2020) Gene fragmentation and RNA editing without borders: eccentric mitochondrial genomes of diplonemids. Nucleic Acids Res **48**:2694–2708

Kaur B, Valach M, Peña-Diaz P, Moreira S, Keeling PJ, Burger G, Lukeš J, Faktorová D (2018) Transformation of *Diplonema papillatum*, the type species of the highly diverse and abundant marine microeukaryotes Diplonemida (Euglenozoa). Environ Microbiol **20**:1030–1040

Keeling PJ, Campo JD (2017) Marine protists are not just big bacteria. Curr Biol **27**:R541–R549

Kent ML, Elston RA, Nerad TA, Sawyer TK (1987) An *Isonema*-like flagellate (Protozoa: Mastigophora) infection in larval geoduck clams, *Panope abrupta*. J Invertebr Pathol **50**:221–229

Kiethega GN, Yan Y, Turcotte M, Burger G (2013) RNA-level unscrambling of fragmented genes in *Diplonema* mitochondria. RNA Biol **10**:301–313

Kivic PA, Walne PL (1984) An evaluation of a possible phylogenetic relationship between the Euglenophyta and Kinetoplastida. Orig Life Evol Biosph **13**:269–288

Kobe B, Kajava AV (2001) The leucine-rich repeat as a protein recognition motif. Curr Opin Struct Biol **11**:725–732

Kostygov AY, Karnkowska A, Votýpka J, Tashyreva D, Maciszewski K, Yurchenko V, Lukeš J (2021) Euglenozoa: taxonomy, diversity and ecology, symbioses and viruses. Open Biol **11**: 200407

Kovářová J, Barrett MP (2016) The pentose phosphate pathway in parasitic trypanosomatids. Trends Parasitol **32**:622–634

Lara E, Moreira D, Vereshchaka A, López-García P (2009) Pan-oceanic distribution of new highly diverse clades of deep-sea diplonemids. Environ Microbiol **11**:47–55

Larsen J, Patterson JL (1990) Some flagellates (Protista) from tropical marine sediments. J Nat Hist **24**:801–937

Lax G, Kolisko M, Eglit Y, Lee WJ, Yubuki N, Karnkowska A, Leander BS, Burger G, Keeling PJ, Simpson AGB (2021) Multigene phylogenetics of euglenids based on single-cell transcriptomics of diverse phagotrophs. Mol Phylogenet Evol **159**: 107088

Lima-Mendez G, Faust K, Henry N, Decelle J, Colin S, Carcillo F, Chaffron S, Ignacio-Espinosa JC, Roux S, Vincent F, Bittner L, Darzi Y, Wang J, Audic S, Berline L, Bontempi G, Cabello AM, Coppola L, Cornejo-Castillo FM, d'Ovidio F, De Meester L, Ferrera I, Garet-Delmas MJ, Guidi L, Lara E, Pesant S, Royo-Llonch M, Salazar G, Sánchez P, Sebastian M, Souffreau C, Dimier C, Picheral M, Searson S, Kandels-Lewis S, Tara Oceans coordinators G, Gorsky G, Not F, Ogata H, Speich S, Stemmann L, Weissenbach J, Wincker P, Acinas SG, Sunagawa S, Bork P, Sullivan MB, Karsenti E, Bowler C, de Vargas C, Raes J (2015) Ocean plankton. Determinants of community structure in the global plankton interactome. Science **348(1262073)**

López-García P, Vereshchaka A, Moreira D (2007) Eukaryotic diversity associated with carbonates and fluid-seawater interface in Lost City hydrothermal field. Environ Microbiol **9**:546–554

López-García P, Rodríguez-Valera F, Pedrós-Alió C, Moreira D (2001) Unexpected diversity of small eukaryotes in deep-sea Antarctic plankton. Nature **409**:603–607

Lukeš J, Wheeler R, Jirsová D, David V, Archibald JM (2018) Massive mitochondrial DNA content in diplonemid and kinetoplastid protists. IUBMB Life **70**:1267–1274

Makiuchi T, Annoura T, Hashimoto M, Hashimoto T, Aoki T, Nara T (2011) Compartmentalization of a glycolytic enzyme in *Diplonema*, a non-kinetoplastid euglenozoan. Protist **162**:482–489

Marande W, Lukeš J, Burger G (2005) Unique mitochondrial genome structure in diplonemids, the sister group of kinetoplastids. Eukaryot Cell **4**:1137–1146

Maslov DA, Yasuhira S, Simpson L (1999) Phylogenetic affinities of *Diplonema* within the Euglenozoa as inferred from the SSU rRNA gene and partial COI protein sequences. Protist **150**:33–42

Massana R, Gobet A, Audic S, Bass D, Bittner L, Boutte C, Chambouvet A, Christen R, Claverie JM, Decelle J, Dolan JR, Dunthorn M, Edvardsen B, Forn I, Forster D, Guillou L, Jaillon O, Kooistra WH, Logares R, Mahé F, Not F, Ogata H, Pawlowski J, Pernice MC, Probert I, Romac S, Richards T, Santini S, Shalchian-Tabrizi K, Siano R, Simon N, Stoeck T, Vaulot D, Zingone A, de Vargas C (2015) Marine protist diversity in European coastal waters and sediments as revealed by high-throughput sequencing. Environ Microbiol **17**:4035–4049

Matthews KR (2015) 25 years of African trypanosome research: From description to molecular dissection and new drug discovery. Mol Biochem Parasitol **200**:30–40

Meek FB, Worthen AH (1865) Contribution to the paleontology of Illinois and other Western States. Proc Acad Nat Sci Philadelph **17**:245–273

Meek FB, Worthen AH (1868) Paleontology. In Worthen AH editor Geological Survey of Illinois **3**. The Legislature of Illinois; Springfield, Illinois, USA, pp 291–565

Montegut-Felkner AE, Triemer RE (1994) Phylogeny of *Diplonema ambulator* (Larsen and Patterson). 1. Homologies of the flagellar apparatus. Europ J Protistol **30**:227–237

Montegut-Felkner AE, Triemer RE (1996) Phylogeny of *Diplonema ambulator* (Larsen and Patterson). 2. Homologies of the feeding apparatus. Europ J Protistol **32**:64–76

Morales J, Hashimoto M, Williams TA, Hirawake-Mogi H, Makiuchi T, Tsubouchi A, Kaga N, Taka H, Fujimura T, Koike M, Mita T, Bringaud F, Concepción JL, Hashimoto T, Embley TM, Nara T (2016) Differential remodelling of peroxisome function underpins the environmental and metabolic adaptability of diplonemids and kinetoplastids. Proc Biol Sci **283**:20160520

Moreira D, López-García P, Rodríguez-Valera F (2001) New insights into the phylogenetic position of diplonemids: G + C content bias, differences of evolutionary rate and a new environmental sequence. Int J Syst Evol Microbiol **51**:2211–2219

Moreira S, Valach M, Aoulad-Aissa M, Otto C, Burger G (2016) Novel modes of RNA editing in mitochondria. Nucleic Acids Res **44**:4907–4919

Morgan-Smith D, Clouse MA, Herndl GJ, Bochdansky AB (2013) Diversity and distribution of microbial eukaryotes in the deep tropical and subtropical North Atlantic Ocean. Deep Sea Res Part **1(78)**:58–69

Mukherjee I, Salcher MM, Andrei AŞ, Kavagutti VS, Shabarova T, Grujčić V, Haber M, Layoun P, Hodoki Y, Nakano SI, Šimek K, Ghai R (2020) A freshwater radiation of diplonemids. Environ Microbiol **22**:4658–4668

Nakazawa M, Hayashi R, Takenaka S, Inui H, Ishikawa T, Ueda M, Sakamoto T, Nakano Y, Miyatake K (2017) Physiological functions of pyruvate:$NADP^+$ oxidoreductase and 2-oxoglutarate decarboxylase in *Euglena gracilis* under aerobic and anaerobic conditions. Biosci Biotechnol Biochem **81**:1386–1393

Nakazawa M, Ando H, Nishimoto A, Ohta T, Sakamoto K, Ishikawa T, Ueda M, Sakamoto T, Nakano Y, Miyatake K, Inui H (2018) Anaerobic respiration coupled with mitochondrial fatty acid synthesis in wax ester fermentation by *Euglena gracilis*. FEBS Lett **592**:4020–4027

Nerad TA (1990) The Life History, Cytology and Taxonomy of *Isonema* and *Isonema*-like Flagellates. University of Maryland; College Park, MD, 259 p Ph.D. Thesis

Obiol A, Giner CR, Sánchez P, Duarte CM, Acinas SG, Massana R (2020) A metagenomic assessment of microbial eukaryotic diversity in the global ocean. Mol Ecol Resour **20**:718–731

Okamoto N, Gawryluk RMR, Del Campo J, Strassert JFH, Lukeš J, Richards TA, Worden AZ, Santoro AE, Keeling PJ (2019) A revised taxonomy of diplonemids including the Eupelagonemidae n. fam. and a type species, *Eupelagonema oceanica* n. gen. & sp. J Eukaryot Microbiol **66**:519–524

Patterson DJ, Vørs N, Simpson AGB, O'Kelly C (2000) Residual Free-living and Predatory Heterotrophic Flagellates. In Lee JJ, Leedale GF, Bradbury P (eds) An Illustrated Guide to the Protozoa. 2nd edn. Society of Protozoologists; Lawrence, Kansas, USA, pp 1302–1328

Pernice MC, Giner CR, Logares R, Perera-Bel J, Acinas SG, Duarte CM, Gasol JM, Massana R (2016) Large variability of bathypelagic microbial eukaryotic communities across the world's oceans. ISME J **10**:945–958

Porter D (1973) *Isonema papillatum* sp. n., a new colorless marine flagellate: a light- and electron microscopic study. J Protozool **20**:351–356

Prokopchuk G, Tashyreva D, Yabuki A, Horák A, Masařová P, Lukeš J (2019) Morphological, ultrastructural, motility and evolutionary characterization of two new Hemistasiidae species. Protist **170**:259–282

Prokopchuk G, Korytář T, Juricová V, Majstorović J, Horák A, Šimek K, Lukeš J (2022) Trophic flexibility of marine diplonemids - switching from osmotrophy to bacterivory. ISME J 2022. https://doi.org/10.1038/s41396-022-01192-0

Reboul G, Moreira D, Annenkova NV, Bertolino P, Vershinin KE, López-García P (2021) Marine signature taxa and core microbial community stability along latitudinal and vertical gradients in sediments of the deepest freshwater lake. ISME J **15**:3412–3417

Roy J, Faktorová D, Benada O, Lukeš J, Burger G (2007) Description of *Rhynchopus euleeides* n. sp. (Diplonemea), a free-living marine euglenozoan. J Eukaryot Microbiol **54**:137–145

Ruinen J (1938) Notizen über Salzflagellaten. II. Über die Verbreitung der Salzflagellaten. Arch Protistenkd **90**:210–258

Sauvadet AL, Gobet A, Guillou L (2010) Comparative analysis between protist communities from the deep-sea pelagic ecosystem and specific deep hydrothermal habitats. Environ Microbiol **12**:2946–2964

Scheckenbach F, Hausmann K, Wylezich C, Weitere M, Arndt H (2010) Large-scale patterns in biodiversity of microbial eukaryotes from the abyssal sea floor. Proc Natl Acad Sci USA **107**:115–120

Scherffel A (1900) *Phaeocystis globosa* nov. spec. nebst einigen Betrachtungen über die Phylogenie niederer, insbesondere brauner Organismen. Wiss Meeresunters Abt Helgoland **4**:1–29

Schnepf E (1994) Light and electron microscopical observations in *Rhynchopus coscinodiscivorus* spec. nov., a color-less, phagotrophic Euglenozoon with concealed flagella. Arch Protistenkd **144**:63–74

Schoenle A, Hohlfeld M, Hermanns K, Mahé F, de Vargas C, Nitsche F, Arndt H (2021) High and specific diversity of protists in the deep-sea basins dominated by diplonemids, kinetoplastids, ciliates and foraminiferans. Commun Biol **4**:501

Schuster FL, Goldstein S, Hershenov B (1968) Ultrastructure of a flagellate *Isonema nigrigricans* nov. gen. nov. sp. from a polluted marine habitat. Protistologica **4**:141–149

Simpson AGB (1997) The identity and composition of the Euglenozoa. Arch Protistenkd **148**:318–328

Simpson AGB, Roger AJ (2004) Protein phylogenies robustly resolve the deep-level relationships within Euglenozoa. Mol Phylogenet Evol **30**:201–212

Simpson AG, Lukeš J, Roger AJ (2002) The evolutionary history of kinetoplastids and their kinetoplasts. Mol Biol Evol **19**:2071–2083

Simpson AG, Gill EE, Callahan HA, Litaker RW, Roger AJ (2004) Early evolution within kinetoplastids (euglenozoa), and the late emergence of trypanosomatids. Protist **155**:407–422

Škodová-Sveráková I, Prokopchuk G, Peña-Diaz P, Záhonová K, Moos M, Horváth A, Šimek P, Lukeš J (2020) Unique dynamics of paramylon storage in the marine euglenozoan *Diplonema papillatum*. Protist **171**: 125717

Škodová-Sveráková I, Záhonová K, Juricová V, Danchenko M, Moos M, Baráth P, Prokopchuk G, Butenko A, Lukáčová V, Kohútová L, Bučková B, Horák A, Faktorová D, Horváth A, Šimek P, Lukeš J (2021) Highly flexible metabolism of the marine euglenozoan protist *Diplonema papillatum*. BMC Biol **19**:251

Skuja H (1948) Taxonomie des Phytoplanktons einiger Seen in Uppland, Schweden. Symb Bot Ups **9**:5–399

Steele MI, Kwong WK, Whiteley M, Moran NA (2017) Diversification of type VI secretion system toxins reveals ancient antagonism among bee gut microbes. mBio **8**: e01630–e1717

Tashyreva D, Prokopchuk G, Votýpka J, Yabuki A, Horák A, Lukeš J (2018a) Life cycle, ultrastructure, and phylogeny of new diplonemids and their endosymbiotic bacteria. mBio **9**: e02447–e2517

Tashyreva D, Prokopchuk G, Yabuki A, Kaur B, Faktorová D, Votýpka J, Kusaka C, Fujikura K, Shiratori T, Ishida KI, Horák A, Lukeš J (2018b) Phylogeny and morphology of new diplonemids from Japan. Protist **169**:158–179

Triemer RE (1992) Ultrastructure of mitosis in *Diplonema ambulator* Larsen and Patterson (Euglenozoa). Europ J Protistol **28**:398–404

Triemer RE, Ott DW (1990) Ultrastructure of *Diplonema ambulator* Larsen & Patterson (Euglenozoa) and its relationship to *Isonema*. Europ J Protistol **25**:316–320

Valach M, Léveillé-Kunst A, Gray MW, Burger G (2018) Respiratory chain Complex I of unparalleled divergence in diplonemids. J Biol Chem **293**:16043–16056

Valach M, Moreira S, Hoffmann S, Stadler PF, Burger G (2017) Keeping it complicated: Mitochondrial genome plasticity across diplonemids. Sci Rep **7**:14166

von der Heyden S, Chao EE, Vickerman K, Cavalier-Smith T (2004) Ribosomal RNA phylogeny of bodonid and diplonemid flagellates and the evolution of euglenozoa. J Eukaryot Microbiol **51**:402–416

Yabuki A, Tame A (2015) Phylogeny and reclassification of *Hemistasia phaeocysticola* (Scherffel) Elbrächter & Schnepf, 1996. J Eukaryot Microbiol **62**:426–429

Yabuki A, Tanifuji G, Kusaka C, Fujikura TK, K, (2016) Hyper-eccentric structural genes in the mitochondrial genome of the algal parasite *Hemistasia phaeocysticola*. Genome Biol Evol **8**:2870–2878

Yabuki A, Kawato M, Nagano Y, Tsuchida S, Yoshida T, Fujiwara Y (2021) Structural comparison of diplonemid communities around the Izu Peninsula, Japan. Microbes Environ **36**:(ME21012)

Yi Z, Berney C, Hartikainen H, Mahamdallie S, Gardner M, Boenigk J, Cavalier-Smith T, Bass D (2017) High-throughput sequencing of microbial eukaryotes in Lake Baikal reveals ecologically differentiated communities and

novel evolutionary radiations. FEMS Microbiol Ecol **93(8)**, fix073

Yubuki N, Edgcomb VP, Bernhard JM, Leander BS (2009) Ultrastructure and molecular phylogeny of *Calkinsia aureus*: cellular identity of a novel clade of deep-sea euglenozoans with epibiotic bacteria. BMC Microbiology **9**:16

Záhonová K, Lax G, Sinha SD, Leonard G, Richards TA, Lukeš J, Wideman JG (2021) Single-cell genomics unveils a canonical origin of the diverse mitochondrial genomes of euglenozoans. BMC Biol **19**:103

Zhou JM, Chai J (2008) Plant pathogenic bacterial type III effectors subdue host responses. Curr Opin Microbiol **11**:179–185